Journal of Limnology

Journal of Limnology 2026; 85:2262
doi:10.4081/jlimnol.2026.2262

Taxonomic survey and DNA barcode library of tardigrades from alpine fens in northwestern Italy

Daniele Camarda,[1] Diego Fontaneto,[2,3,4] Daniel Bajorek,[5] Oscar Lisi,[1] Daniel Stec[2,5*]

[1]Department of Biological, Geological and Environmental Sciences, Section of Animal Biology, University of Catania, Italy; [2]Molecular Ecology Group (MEG), Water Research Institute (IRSA), National Research Council of Italy (CNR), Verbania-Pallanza, Italy; [3]National Biodiversity Future Center, Palermo, Italy; [4]University of Fribourg, Fribourg, Switzerland; [5]Institute of Systematics and Evolution of Animals of the Polish Academy of Sciences, Kraków, Poland

Abstract

Peatlands and peatland-like habitats are among the most vulnerable ecosystems to climate change. Owing to their specific microclimatic conditions, which maintain high and stable moisture levels, they host assemblages dominated by hydrophilous taxa, including several groups of mostly freshwater tardigrades. Despite this, tardigrade diversity in peat-related habitats remains poorly known. Here, we conducted an extensive taxonomic survey of tardigrades based on 35 samples collected from alpine fens in northern Italy. We detected 30 species-level tardigrade taxa, of which 23 were successfully DNA barcoded. One species of the genus *Crenubiotus* is new to science and is formally described herein as *Crenubiotus meg* sp. nov. We also provide updated morphological and taxonomic information for two enigmatic taxa, *Fontourion secchii* and *Microhypsibius minimus*, which have long been hindered by data deficiency. Notably, the assemblage recovered comprises several taxa with boreo-alpine or cold-adapted affinities, highlighting alpine peatlands as potential refugial habitats for relict tardigrade lineages. In addition, we performed phylogenetic analyses to resolve the placement of the newly described *Crenubiotus* species and to clarify the relationships of four *Murrayon* lineages recovered in this study. This work represents the first integrative taxonomic inventory of tardigrades inhabiting peat-like habitats and contributes an extensive, curated set of reference DNA sequences for this understudied habitat. These data provide an essential foundation for high-throughput biodiversity assessments using mega- and metabarcoding approaches and offer new insights into tardigrade taxonomy and evolutionary relationships.

Key words: alps; biodiversity; meiofauna; DNA barcoding; *Sphagnum*; Tardigrada.

Correspondence to: daniel_stec@interia.eu

Introduction

Fens and peat bogs are among the most threatened habitats in Europe (Moore, 2002). They are protected in many countries for their exceptional biodiversity and their vital function as natural carbon sinks. Yet these ecosystems are under growing pressure from human activity, grazing by introduced hoofed animals, invasive plants, wildfires, and these threats are likely to intensify with climate change. As a result, they have become the focus of wide-ranging conservation efforts across Europe (Nordbeck and Hogl, 2023). Successful restoration, however, depends on understanding the tight interplay between abiotic and biotic factors (Rowland *et al.*, 2021). The fragile balance of these systems has led to predictions that many peatlands, especially those at higher elevations, may disappear in the coming decades (Antala *et al.*, 2022). This decline is closely tied to the loss of species, one of the most profound outcomes of human caused global change (Cowie *et al.*, 2022). Tracking such changes in biodiversity requires solid reference points and reliable knowledge of species composition and this might be a challenge for many overlooked groups of microscopic metazoans with notoriously complex taxonomy (Martínez *et al.*, 2025).

One such group is Tardigrada, a phylum of micrometazoans that, together with Onychophora and Arthropoda, forms the superclade Panarthropoda (Nielsen, 2011; Wu *et al.*, 2023). Tardigrades occupy a wide range of environments, including freshwater, marine, and terrestrial habitats (Nelson *et al.*, 2019). The terrestrial species are the most familiar, typically inhabiting the thin films of water that coat mosses, lichens, algae, leaf litter, and soil. They remain active only when at least a minimal layer of moisture is present on the substrate (Nelson *et al.*, 2019). Tardigrades are famous for their ability to survive extreme environmental conditions, such as desiccation (Wełnicz *et al.*, 2011), due to their cryptobiotic capabilities, which are generally more pronounced in limno-terrestrial than in aquatic taxa (Guidetti *et al.*, 2011). Although they have captured public attention as some of the toughest animals on Earth (Guidetti *et al.*, 2012), they still remain understudied, with their taxonomy being very challenging. This is largely due to the scarcity of informative morpholog-

ical characters and the prevalence of cryptic or pseudocryptic diversity (Kosztyła *et al.*, 2016; Morek *et al.*, 2021; Surmacz *et al.*, 2025c).

Currently, more than 1,500 tardigrade species have been described, the vast majority from terrestrial habitats (Degma and Guidetti, 2025). Reviews of freshwater tardigrade diversity indicate that hydrophilous taxa constitute only about 10% of the known species (excluding marine ones; McFatter *et al.*, 2007; Garey *et al.*, 2008; Kayastha *et al.*, 2021). These studies explicitly demonstrate that the primary focus related to aquatic tardigrades was directed on lotic and lentic systems. However, to our knowledge, there has been no dedicated species-level taxonomic or faunistic survey of tardigrades inhabiting wetland ecosystems such as peat bogs and fens, which represent intermediate environments between terrestrial and aquatic habitats and host predominantly hydrophilous tardigrade species. Although tardigrades have occasionally been reported from these environments, such findings have typically come from opportunistic or non-targeted sampling (e.g., Ramazzotti and Maucci, 1983; Kayastha *et al.*, 2021).

Interestingly, other meiofaunal groups that commonly dwell together with tardigrades in the same habitats, have received more attention in peatland studies, such as rotifers (Bielańska-Grajner *et al.*, 2011; Fontaneto *et al.*, 2019), nematodes (Renčo *et al.*, 2025), and gastrotrichs (Kisielewski, 1981; Kisielewska, 1982). Recently, tardigrades from peatland environments in Finland have been investigated in ecological community studies, revealing substantial heterogeneity in community composition and highlighting the joint influence of micro- and macroenvironmental factors shaping their assemblages (Mäenpää *et al.*, 2023, 2024, 2025). Nonetheless, despite the considerable sampling effort in these Finnish studies, taxonomic identifications were restricted to the genus level, highlighting the persistent difficulties and time-consuming nature of achieving reliable species-level resolution in tardigrade taxonomy (Surmacz *et al.*, 2025c). Importantly, these findings demonstrate that peatlands represent a promising system for studying environmental heterogeneity in tardigrade communities, but advancing our understanding will require deeper, species-level taxonomic resolution.

To address this knowledge gap, we conducted an integrative taxonomic survey of tardigrades inhabiting poor fens with patches of intermediate fen–bog vegetation in northern Italy. This habitat can be characterised as minerotrophic peatlands with low nutrient availability and weak groundwater influence, often transitional toward ombrotrophic bog conditions (Rydin and Jeglum, 2006). We sampled mosses from alpine and subalpine *Sphagnum*-rich fens in the Piedmont region and performed detailed morphological examinations using light and scanning electron microscopy to document the species present. These data were complemented with sequences from four molecular markers commonly used in tardigrade taxonomy (COI, 18S rRNA, 28S rRNA and ITS-2), together constituting the first morpho-molecular reference library of tardigrades from alpine poor fens, and providing a baseline for future biodiversity assessments using DNA barcoding or metabarcoding. In addition to the faunistic inventory, several taxa of particular systematic relevance (most notably a new species of *Crenubiotus* Lisi, Londoño & Quiroga, 2020 and lineages within *Murrayon* Bertolani & Pilato, 1988) were subjected to targeted phylogenetic analyses. Finally, three species for which our material offered substantial new diagnostic insight received expanded taxonomic treatments, which are presented in detail in this contribution.

Methods

Sample collection and processing

Samples of wet mosses were collected from alpine and subalpine fens by DS, DB, and DF in five areas spanning the elevation from 837 to 2361 m asl. Collection data for the 35 samples analysed in this study and collected in five distinct areas are provided in Tab. 1. All samples were collected in Italy except for one sample collected in Switzerland near the Italian border. The Italian sampling sites were located within the protected area Aree Protette dell'Ossola, and the appropriate collection permits were obtained. The Swiss locality was situated outside protected areas. Each sample consisted of approximately 0.5 kg of wet moss, collected into 1.5 L plastic zip-lock bags. All samples were transported to the laboratory at CNR-IRSA and processed either on the same day or stored in the fridge and processed the following day. In the laboratory, each sample was washed and sieved through a set of sieves with mesh sizes of 500 µm, 250 µm, and 36 µm. Material retained on the finest sieve (36 µm) was washed into Falcon tubes and frozen for later examination. A subsample of each moss sample (approximately 25%) was dried and sent to a bryophyte specialist for species identification. Moss species identified for each sample are listed in Tab. 1. Aliquots of the mixed material were transferred to Petri dishes and examined under a stereomicroscope. Tardigrade specimens (animals and eggs) were isolated using a glass pipette or an Irwin loop. No more than ten Petri dishes were checked per sample during this phase of the study. All extracted specimens were mounted in permanent slides for examination under light microscope (LM). The extraction procedure was later repeated for selected samples to obtain additional specimens for scanning electron microscopy (SEM) and for DNA extraction. Since our study reports multiple tardigrade genera whose names begin with the same letter, we used genus abbreviations following the conventions proposed by Perry *et al.* (2019).

Microscopy and imaging

Specimens (animals and eggs) designated for light microscopy analysis were mounted on permanent slides using Hoyer's medium. Slides were dried for three days in 50°C and sealed with nail polish before examination. Observations were performed using a ZEISS Axio A1 microscope equipped with both phase-contrast (PCM) and differential interference contrast (DIC), collectively called light contrast microscopy (LCM). Photomicrographs were taken with DLT-Cam PRO 20 MP digital cameras. For scanning electron microscopy (SEM), specimens were processed following the protocol of Camarda *et al.* (2024) and sputter-coated with gold. The SEM imaging was conducted using a Phenom XL G2 microscope at the University of Catania, Italy. For structures that could not be fully focused on a single light microscope photograph, a series of images were taken and then assembled into a single deep-focus image using GIMP v3.0.6 (The GIMP Development Team, 2019).

Morphometrics and morphological nomenclature

All measurements of tardigrade structures are given in µm. Morphometric data were recorded only when structures were undamaged, clearly visible, and properly oriented. The classification and terminology of the buccal apparatus and claw types follow Pilato and Binda (2010) and Gąsiorek and Michalczyk (2020).

Tab. 1. Information about the samples examined in this study. A map depicting the five investigated areas is provided in *Supplementary Materials SM.06*.

Sample code	Area	Locality	Latitude	Longitude	Collection date	Moss ID
BOG.001	A1	Valle Bognanco - Torbiera di Gattascosa	46.156975	8.170665	28.10.2023	*Palustriella falcata* (Brid.) Hedenäs
BOG.002	A1	Valle Bognanco - Torbiera di Gattascosa	46.15697	8.170665	28.10.2023	*Sphagnum teres* (Schimp.) Ångstr.
BOG.003	A1	Valle Bognanco - Torbiera di Gattascosa	46.157052	8.170827	28.10.2023	*Sphagnum medium* Limpr.
BOG.004	A1	Valle Bognanco - Torbiera di Gattascosa	46.159199	8.157767	28.10.2023	*Sphagnum fallax* (H.Klinggr.) H.Klinggr.
BOG.005	A1	Valle Bognanco - Torbiera di Gattascosa	46.159206	8.157822	28.10.2023	*Sphagnum compactum* Lam. & DC.
BOG.006	A1	Valle Bognanco - Torbiera di Gattascosa	46.159323	8.157558	28.10.2023	*Sphagnum fallax* (H.Klinggr.) H.Klinggr.
BOG.007	A1	Valle Bognanco - Torbiera di Gattascosa	46.160167	8.157081	28.10.2023	*Sphagnum compactum* Lam. & DC.
BOG.008	A1	Valle Bognanco - Torbiera di Gattascosa	46.160288	8.157063	28.10.2023	*Sphagnum girgensohnii* Russow
BOG.009	A1	Valle Bognanco - Torbiera di Gattascosa	46.160283	8.157013	28.10.2023	*Sphagnum subsecundum* Nees
BOG.010	A1	Valle Bognanco - Torbiera di Gattascosa	46.16178	8.158211	28.10.2023	*Sphagnum compactum* Lam. & DC.
BOG.011	A1	Valle Bognanco - Torbiera di Gattascosa	46.161768	8.158257	28.10.2023	*Sphagnum medium* Limpr.
BOG.012	A1	Valle Bognanco - Torbiera di Gattascosa	46.161728	8.15826	28.10.2023	*Sphagnum compactum* Lam. & DC.
BOG.013	A1	Valle Bognanco - Torbiera di Gattascosa	46.152389	8.191218	28.10.2023	*Sphagnum warnstorfii* Russow *Sphagnum compactum* Lam. & DC.
BOG.014	A1	Valle Bognanco - Torbiera di Gattascosa	46.152306	8.191412	28.10.2023	*Sphagnum angustifolium* (C.E.O.Jensen ex Russow) C.E.O.Jensen
BOG.015	A1	Valle Bognanco - Torbiera di Gattascosa	46.152423	8.191172	28.10.2023	*Sphagnum medium* Limpr.
BOG.01.3	A2	Torbiera di Valle Scoccia	45.875297	8.489676	24.09.2024	*Sphagnum palustre* L. *Sphagnum fallax* (H.Klinggr.) H.Klinggr.
BOG.02.2	A2	Torbiera di Valle Scoccia	45.875219	8.489525	24.09.2024	*Sphagnum fallax* (H.Klinggr.) H.Klinggr.
BOG.03.3	A2	Torbiera di Valle Scoccia	45.875387	8.489211	24.09.2024	*Sphagnum palustre* L.
BOG.04.4	A2	Torbiera di Valle Scoccia	45.875673	8.488558	24.09.2024	*Sphagnum palustre* L.
BOG.05.1	A2	Torbiera di Valle Scoccia	45.876779	8.487257	24.09.2024	*Sphagnum fallax* (H.Klinggr.) H.Klinggr.
BOG.06.4	A3	Passo San Giacomo	46.459701	8.453291	25.09.2024	*Climacium dendroides* (Hedw.) F.Weber & D.Mohr
BOG.07.1	A3	Valle Formazza - Passo San Giacomo	46.45844	8.451108	25.09.2024	*Limprichtia cossonii* (Schimp.) L.E.Anderson; *Palustriella falcata* (Brid.) Hedenäs; *Bryum pseudotriquetrum* (Hedw.) P.Gaertn., B.Mey. & Schreb.
BOG.08.4	A3	Valle Formazza - Passo San Giacomo	46.457763	8.449069	25.09.2024	*Palustriella falcata* (Brid.) Hedenäs *Philonotis fontana* (Hedw.) Brid.
BOG.09.3	A3	Valle Formazza - Maria Luisa	46.432439	8.430294	25.09.2024	*Bryum schleicheri* Schwägr.
BOG.10.5	A3	Valle Formazza - Torbiera di Valgeis	46.430007	8.42394	25.09.2024	*Sphagnum subsecundum* Nees
BOG.11.3	A4	Valle Antrona - Alpe Lareccio	46.022573	8.063325	27.09.2024	*Sphagnum compactum* Lam. & DC. *Sphagnum subsecundum* Nees
BOG.12.1	A4	Valle Antrona - Alpe Lareccio	46.024242	8.066623	27.09.2024	*Sphagnum subsecundum* Nees
BOG.13.3	A4	Valle Antrona - Alpe Lareccio	46.026836	8.069292	27.09.2024	*Sphagnum fallax* (H.Klinggr.) H.Klinggr.
BOG.14.5	A4	Valle Antrona - Alpe Larcero	46.030302	8.074791	27.09.2024	*Sphagnum russowii* Warnst. *Sphagnum palustre* L. *Straminergon stramineum* (Dicks. ex Brid.) Hedenäs
BOG.15.2	A4	Valle Antrona - Alpe Larcero	46.030272	8.076961	27.09.2024	*Sphagnum girgensohnii* Russow
BOG.21.3	A5	Valle Vigezzo - Lago Panelatte	46.200819	8.45623	30.09.2024	*Sphagnum compactum* Lam. & DC.
BOG.22.5	A5	Valle Onsernone - laghetto a Alpe Galeria	46.203006	8.467643	30.09.2024	*Sphagnum compactum* Lam. & DC.
BOG.23.2	A5	Valle Onsernone - Alpe Galeria	46.20491	8.465245	30.09.2024	*Sphagnum girgensohnii* Russow
BOG.24.5	A5	Valle Vigezzo - San Pantaleone	46.197216	8.462932	30.09.2024	*Sphagnum russowii* Warnst.; *Sphagnum subsecundum* Nees; *Straminergon stramineum* (Dicks. ex Brid.) Hedenäs
BOG.25.3	A5	Valle Vigezzo - Alpe i Motti	46.194365	8.463157	30.09.2024	*Sphagnum fallax* (H.Klinggr.) H.Klinggr.

Body length was measured from the anterior extremity to the posterior end of the body, excluding the hind legs. Claw measurements follow the methodology of Kaczmarek and Michalczyk (2017), Guidetti *et al.* (2016), and Beasley *et al.* (2008). The macroplacoid length sequence is given according to Kaczmarek *et al.* (2014), whereas the morphological states of cuticular bars on the legs follow Kiosya *et al.* (2021) and Gąsiorek *et al.* (2024). Buccal tube length and the level of the stylet support insertion point were measured following Pilato (1981). The *pt* index represents the ratio of the length of a given structure to the length of the buccal tube, expressed as a percentage (Pilato, 1981). Morphometric datasets were processed using the "Parachela" v.1.8 template provided by the Tardigrada Register (Michalczyk and Kaczmarek, 2013). Morphometric measurements were obtained for three species that needed to receive detailed taxonomic treatment and are provided in the Supplementary Materials (SM.01-03).

DNA extraction and sequencing

Specimens designated for molecular analyses were first examined *in vivo* under a light microscope to confirm their identification. Hologenophores were prepared by photo-vouchering each individual prior to extraction, following the procedure of Cesari *et al.* (2011). For *Murrayon* taxa investigated in this study as well as for *Mesobiotus* aff. *furciger* all voucher specimens were constituted by eggs. Total genomic DNA was extracted from single specimens using the Chelex® 100 resin protocol (Bio-Rad) described by Casquet *et al.* (2012), with modifications outlined in Stec *et al.* (2020a). Molecular markers included fragments of the small and large ribosomal subunits (18S and 28S rRNA), the nuclear internal transcribed spacer 2 (ITS-2), and the mitochondrial cytochrome c oxidase subunit I (COI) gene. The aim of this part of the study was to maximize the recovery of COI and 18S rRNA sequences for each morphospecies identified in the previous phase, while also sequencing the additional markers (28S rRNA and ITS-2) for several taxonomically unusual or noteworthy taxa. Amplification and sequencing of all fragments followed the procedures described in Stec *et al.* (2020a). Primer sets used for each gene region are listed in Supplementary Materials (SM.04). Sequencing was performed on an ABI PRISM 3130xl Genetic Analyzer (Applied Biosystems, Waltham, MA, USA). Raw chromatograms were edited and assembled in MEGA12 (Kumar *et al.* 2024). The COI sequences were translated into amino acids in MEGA12 to screen for pseudogenes and stop codons. All newly obtained sequences were deposited in GenBank; accession numbers for each vouchered specimen are provided in Supplementary Materials (SM.04).

Species delimitation and genetic analyses

To assess the presence of putative cryptic species in the newly sampled material, we prepared a COI alignment including all newly obtained sequences and applied the ASAP species-delimitation method (Assemble Species by Automatic Partitioning; Puillandre *et al.*, 2021). Analyses were run under default settings using the JC69 substitution model. Results of the species delimitation analyses are provided in Supplementary Materials (SM.05). To assess whether the COI sequences obtained in this study correspond to lineages already represented in public databases, we performed BLAST searches using the NCBI Basic Local Alignment Search Tool (BLAST; Altschul *et al.*, 1990). For each putative species recovered in our dataset by ASAP, a representative COI sequence was queried against the NCBI core_nt database (Sayers *et al.*, 2026) with blastn (Camacho *et al.*, 2009) using default parameters. Hits were considered to match our sequences when the pairwise identity exceeded 97%, a threshold commonly applied as an approximate species boundary in tardigrade DNA barcoding (Cesari *et al.*, 2013; Surmacz *et al.*, 2025c). The list of matches is provided in Supplementary Materials (SM.05).

Phylogenetic analyses were conducted to determine the position of newly discovered populations belonging to the genera *Crenubiotus* and *Murrayon*. The analyses used the DNA sequence dataset compiled by Stec *et al.* (2020c), supplemented with newly published sequences (Guidetti *et al.*, 2021, 2022; Stec and Morek, 2022; Vecchi *et al.*, 2022, 2025; Stec, 2023; Massa *et al.*, 2024; Zhang *et al.*, 2024; Camarda *et al.*, 2025a; Flores-Romero *et al.*, 2025) and with the sequences obtained in the present study. A complete list of GenBank accession numbers for both newly generated and downloaded sequences used in phylogenetic analyses is provided in Supplementary Materials (SM.04). Sequence alignments were generated in MAFFT v7 (Katoh *et al.*, 2002; Katoh and Standley, 2013). Ribosomal markers (18S and 28S rRNA) were aligned using the Q-INS-i algorithm, which incorporates RNA secondary structure. Protein-coding (COI) and ITS-2 sequences were aligned using the "auto" strategy. All alignments were visually inspected and manually adjusted where necessary. Final alignment lengths were 830 bp (18S rRNA), 824 bp (28S rRNA), and 658 bp (COI). Because ITS-2 typically contains highly variable and ambiguously aligned regions, the initial ITS-2 alignment was refined using GBlocks v0.91b (Castresana, 2000) under the "less stringent" settings. The resulting ITS-2 matrix was 214 bp in length. Concatenated datasets were assembled in SequenceMatrix v1.8 (Vaidya *et al.*, 2011) under a four-partition scheme (18S + 28S + ITS-2 + COI). Maximum likelihood (ML) phylogenetic analyses and model selection were performed in IQ-TREE v2 (Nguyen *et al.*, 2015; Trifinopoulos *et al.*, 2016) using the W-IQ-TREE web interface. Optimal substitution models for each partition were inferred with ModelFinder. Branch support was estimated with 1,000 ultrafast bootstrap replicates (Hoang *et al.*, 2018). Bayesian inference (BI) analyses were conducted in MrBayes v3.2 (Ronquist and Huelsenbeck, 2003). Partitioning schemes and substitution models were selected using PartitionFinder2 (Lanfear *et al.*, 2017). Two parallel runs, each consisting of one cold and three heated chains, were executed for 15 million generations with sampling every 1,000 generations. Convergence was assessed by monitoring the average standard deviation of split frequencies (<0.01) and by inspecting posterior distribution diagnostics in Tracer v1.7 (Rambaut *et al.*, 2018). All effective sample size (ESS) values exceeded 200. The first 10% of sampled trees were discarded as burn-in, and a majority-rule consensus tree was generated. The consensus tree was viewed and visualised by FigTree v.1.4.3 available from http://tree.bio.ed.ac.uk/software/figtree. Raw ML and BI trees in newick format are provided in Supplementary Materials (SM.04).

Additionally, to assess the genetic distinctiveness of the population of *Fontourion* Gąsiorek, Morek & Michalczyk 2024 discovered in this study, we downloaded COI sequences of the three other described *Fontourion* species (*Fontourion glaciale* (Zawierucha, Buda & Gąsiorek, 2020), *Fontourion islandicum* (Buda & Zawierucha, 2018), and *Fontourion recamieri* (Richters, 1911)) as published in their original descriptions or redescriptions (Gąsiorek *et al.*, 2017; Buda *et al.*, 2018; Zawierucha *et al.*, 2020). These sequences, together with the COI sequences obtained in the present study, were aligned in MAFFT v7 following the procedure described above. The resulting alignment (683 bp) was imported into MEGA

12 (Kumar *et al.*, 2024), where a neighbour-joining tree was constructed with 1000 bootstraps to visualise divergence among the four taxa, and uncorrected p-distances were calculated to quantify pairwise genetic divergence. The results of these analyses are provided in Supplementary Materials (SM.05).

Results

Faunistic summary

Of the 35 samples of the five areas examined in this study, only one (BOG.005) contained no tardigrades or eggs. Specimens extracted from the remaining 34 samples were mounted on 166 permanent slides, comprising 700 animals, 206 eggs, and 6 exuviae. Examination of these slides revealed 25 species-level taxa diagnosed based on morphology (Tab. 2). An additional three taxa were detected exclusively through DNA barcoding, as no voucher material for these could have been mounted on permanent slides (Tab. 2). It is not possible to determine whether *Diphascon* sp. 1 recovered by morphology based on the material mounted in slides corresponds to the *Diphascon* sp. detected only through DNA. These lineages were therefore treated conservatively as a single species for final census. Species-delimitation analyses (details below) further indicated that three morphologically recognised taxa (*Murrayon* cf. *pullari*, *Murrayon* cf. *hastatus*, and *Thulinius* cf. *saltursus*) each comprise two putative cryptic species. Incorporating these cryptic lineages and treating the *Diphascon* Plate, 1888 taxa conservatively as one increases the total number of species detected in this study to 30.

Species-level identification was frequently not possible in two genera: *Murrayon* and *Mesobiotus* Vecchi, Cesari, Bertolani, Jönsson, Rebecchi & Guidetti, 2016. Animals of *Mur.* cf. *hastatus* and *Mur.* cf. *pullari* cannot be reliably distinguished due to high morphological similarity and their common co-occurrence within the same samples. Consequently, all *Murrayon* animals were identified as *Murrayon* sp., whereas records of *Mur.* cf. *pullari* and *Mur.* cf. *hastatus* in this study are based solely on egg morphology. In the genus *Mesobiotus*, species diagnoses rely heavily on egg ornamentation; many samples contained only animals, preventing species-level identification (Supplementary Materials SM.05).

Tab. 2. Species-level presence/absence data for each study area (see Tab. 1). "M" in the last column indicates validation by morphological examination of specimens mounted in permanent slides, while "DNA" indicates genetic validation. Asterisks denote three taxa that each comprise two cryptic species recognized with genetic analyses, but are not split in the species occurrence data set based on morphological examination. The five investigated areas are labelled A1–A5. Detailed presence/absence data per each examined sample is provided in *Supplementary Materials SM.05*.

Taxon	A1	A2	A3	A4	A5	Validation
Adropion scoticum	X	X	X	X	X	M + DNA
Adropion cf. *scoticum*	X	X		X		M + DNA
Adropion sp. 1	X	X				M + DNA
Arctodiphascon sp.	X					DNA
Borealibius zetlandicus					X	M + DNA
Crenubiotus meg sp. nov.	X			X	X	M + DNA
Cucumibius annulatus	X		X			M + DNA
Dianea sp.	X					DNA
Dianea cf. *costata*		X	X		X	M + DNA
Diphascon sp. 1	X	X	X			M
Diphascon sp.		X				DNA
Fontourion secchi	X		X			M + DNA
Guidettion sp. 1	X					M
Hypsibius cf. *repentinus*	X	X	X			M + DNA
Hypsibius sp. 1	X		X			M + DNA
Isohypsibius sp. 1	X		X	X		M
Macrobiotus hufelandi	X			X		M + DNA
Macrobiotus cf. *hufelandi*	X			X		M + DNA
Mesobiotus aff. *furciger*	X					M + DNA
Mesobiotus aff. *harmsworthi* sp.1	X	X				M
Mesobiotus aff. *harmsworthi* sp.2			X			M
Microhypsibius minimus			X	X	X	M + DNA
Murrayon cf. *hastatus**	X	X	X	X	X	M + DNA
Murrayon cf. *pullari**	X	X	X		X	M + DNA
Paramacrobiotus sp. 1			X			M
Pilatobius cf. *bullatus*	X					M
Pilatobius cf. *rugosus*	X				X	M + DNA
Thulinius cf. *saltursus**	X		X	X		M + DNA

Across the 34 samples that contained fauna, species richness ranged from 1 to 9 taxa, with most samples yielding 3-6 taxa (Supplementary Materials SM.05). At the genus level, the assemblage was dominated numerically by *Crenubiotus*, *Murrayon*, *Fontourion*, *Thulinius* Bertolani, 2003, *Pilatobius* Bertolani, Guidetti, Marchioro, Altiero, Rebecchi & Cesari, 2014 and *Microhypsibius* Thulin, 1928, which together accounted for the majority of specimens recovered. A new *Crenubiotus* species was the most abundant taxon, with over 200 specimens (animals + eggs combined), recorded in 10 samples. The *Murrayon* records also dominated numerically: *Mur.* cf. *pullari* (63 eggs in 16 samples), *Mur.* cf. *hastatus* (61 eggs in 13 samples), and *Murrayon* sp. (60 animals in 18 samples). Other moderately abundant and widespread taxa included *Fontourion secchi* (Bertolani & Rebecchi, 1996) (89 individuals, 7 samples), *Thulinius* cf. *saltursus* (90 individuals, 4 samples), *Mesobiotus* sp. (25 individuals, 9 samples), *Hypsibius* cf. *repentinus* (25 individuals, 5 samples), *Pilatobius* cf. *rugosus* (35 individuals, 9 samples), *Microhypsibius minimus* Kristensen, 1982 (29 individuals, 3 samples), and *Adropion scoticum* (Murray, 1905) (18 individuals, 13 samples). Several taxa were rare, being represented by only a few individuals or restricted to a single sample. These include *Borealibius zetlandicus* (Murray, 1907), *Cucumibius annulatus* (Murray, 1905), *Hypsibius* sp. 1, *Adropion* cf. *scoticum*, *Mesobiotus* aff. *furciger*, *Mesobiotus* aff. *harmsworthi* sp. 1 and sp. 2, *Isohypsibius* sp. 1, *Dianea* cf. *costata*, *Paramacrobiotus* sp. 1, *Diphascon* sp. 1, *Guidettion* sp. 1, *Adropion* sp. 1, and *Pilatobius* cf. *bullatus* (Supplementary Materials SM.05). Although some differences in taxa occurrences among samples were observed, the sampling design and extraction procedures were not standardised for quantitative community analysis. Accordingly, we refrain from interpreting these patterns ecologically and present the data strictly as a qualitative faunistic inventory.

DNA barcoding and species delimitation

We successfully amplified and sequenced DNA from 48 specimens, yielding 48 COI, 32 18S rRNA, 19 28S rRNA, and 17 ITS-2 sequences. All voucher-specimen codes and their corresponding GenBank accession numbers are listed in Supplementary Materials SM.04. The ASAP species-delimitation analyses produced ten alternative partitions, suggesting between 13 and 27 putative species in the dataset (Supplementary Materials SM.05). Partition 1 had the lowest ASAP score (3.0) but merged *Macrobiotus hufelandi* C.A.S. Schultze, 1834 and *Macrobiotus* cf. *hufelandi* into a single species-level unit. Because these taxa are treated as distinct in tardigrade systematics (Bertolani *et al.*, 2011; Surmacz *et al.*, 2025b), we did not adopt this solution. Instead, we selected Partition 3, which had the lowest ASAP score among the partitions retaining these taxa as separate lineages. This partition delimited 23 putative species, including three morphologically defined taxa that each comprised two putative species that were mentioned above: *Thu.* cf. *saltursus*, *Mur.* cf. *hastatus*, and *Mur.* cf. *pullari* (Supplementary Materials SM.05). Overall, molecular data were largely congruent with morphological identifications, with all analysed morphospecies forming distinct genetic clusters except in these three cases where COI barcoding revealed the presence of putative cryptic species.

BLAST searches showed that only seven of the 23 putative species had close matches (≥97% identity) to sequences archived in GenBank. These were *Murrayon* cf. *pullari* sp. 2, *Mac.* cf. *hufelandi*, *Mac. hufelandi*, *Hypsibius* sp., *Cuc. annulatus*, *Bor. zetlandicus*, and *Adr. scoticum* (Supplementary Materials SM.05). The remaining 16 putative species (70%) lacked close matches, indicating that the present study provides the first reliable COI barcodes for these lineages. One unexpected result arose from a COI sequence obtained from an ovoid egg bearing mushroom-shaped processes typical of the *Mac. hufelandi* morphogroup. The BLASTn identified this sequence as belonging to a rotifer, with the closest hit being *Lecane cornuta* (Müller, 1786) (JX216679; 79.20% identity), while BLASTx indicated highest similarity to *Cephalodella gibba* (Ehrenberg, 1830) of the family Notommatidae (AAP45040; 92.73% identity of the protein sequence). Given the remarkable morphological convergence between these rotifer eggs and the ornamented eggs of the *hufelandi* morphogroup, we provide their photographic documentation in Supplementary Materials SM.06.

Phylogenetic analysis

Phylogenetic analyses in this study focused on taxa for which resolving evolutionary placement was essential for accurate taxonomic interpretation. First, the newly discovered *Crenubiotus* population represents a species new to science and therefore required formal placement within Macrobiotoidea to support its description. Second, our material included two *Murrayon* lineages identified as *Murrayon* cf. *hastatus*, providing the first molecular data relevant to the systematic uncertainty surrounding *Murrayon hastatus* (Murray, 1907), a species exhibiting morphological traits partly consistent with *Paramurrayon* Guidetti, Giovannini, Del Papa, Ekrem, Nelson, Rebecchi & Cesari, 2022. To address these issues, we assembled a targeted multi-marker dataset for the superfamily Macrobiotoidea, combining our sequences with available published data, and inferred phylogenetic relationships using both maximum-likelihood (ML) and Bayesian inference (BI).

Both ML and BI analyses yielded highly congruent topologies (Fig. 1; Supplementary Materials SM.04). The relationships among families within Macrobiotoidea were consistent with previous studies (Stec *et al.*, 2020c, 2021; Guidetti *et al.*, 2021, 2022). The family Adorybiotidae was recovered as comprising two genera, *Adorybiotus* Maucci & Ramazzotti, 1981 and *Crenubiotus*. The latter is of particular relevance here, as it includes the new *Crenubiotus* species identified in this study along with five congeners. The new species formed a clade with *Crenubiotus salishani* Vecchi, Choong & Calhim, 2022 (Canada) and *Crenubiotus liangshuiensis* J.-Y. Zhang, X.-L. Sun, N. Wang, Hao, Ma, N. Zhao, H. Li, M. Zhao & S.-T. Yang, 2024 (China), although relationships within this clade received only weak support. Notably, the type species *Crenubiotus crenulatus* (Richters, 1904) is represented in our dataset only by ribosomal markers because its nominal COI sequence was found to belong to *Mesobiotus* (likely due to contamination) as already reported during tardigrade COI database curation by (Surmacz *et al.*, 2025c).

The family Murrayidae was recovered as comprising its three recognized genera (*Dactylobiotus* R.O. Schuster, 1980, *Murrayon*, and *Paramurrayon*), which however formed four distinct clusters (Fig. 1). *Dactylobiotus* resolved into two major clades, broadly consistent with the proposed division into species with and without dorso-lateral papillae (Camarda *et al.*, 2025b). In contrast, *Murrayon* was recovered as polyphyletic. Two well-defined clusters were observed: one consisting of several poorly identified populations of *Mur. pullari* or *Mur. cf. pullari* from Scotland, Italy, and Greenland, forming a sister-group relationship with *Dactylobiotus*; and a second cluster comprising two putative cryptic species of *Murrayon* cf. *hastatus* from Italy sequenced in this study. Remarkably, this latter group formed a strongly supported monophyletic clade placed as sister to *Paramurrayon*, providing the first molecular evidence relevant to the ambiguous systematic position of *Mur. hastatus*.

Taxonomic account

Detailed taxonomic treatments were prepared only for those taxa for which the newly collected material provided substantial new information or resolved previously unresolved problems. These include: i) a new species of *Crenubiotus*, whose diagnosis and description are presented here for the first time; ii) *Fontourion secchi*, regarded for a few years as a *species inquirenda* (Gąsiorek *et al.*, 2017), for which our material enables clarification and description update; and iii) *Microhypsibius minimus*, a rarely reported and poorly characterised species from a very enigmatic genus whose existing descriptions are fragmentary.

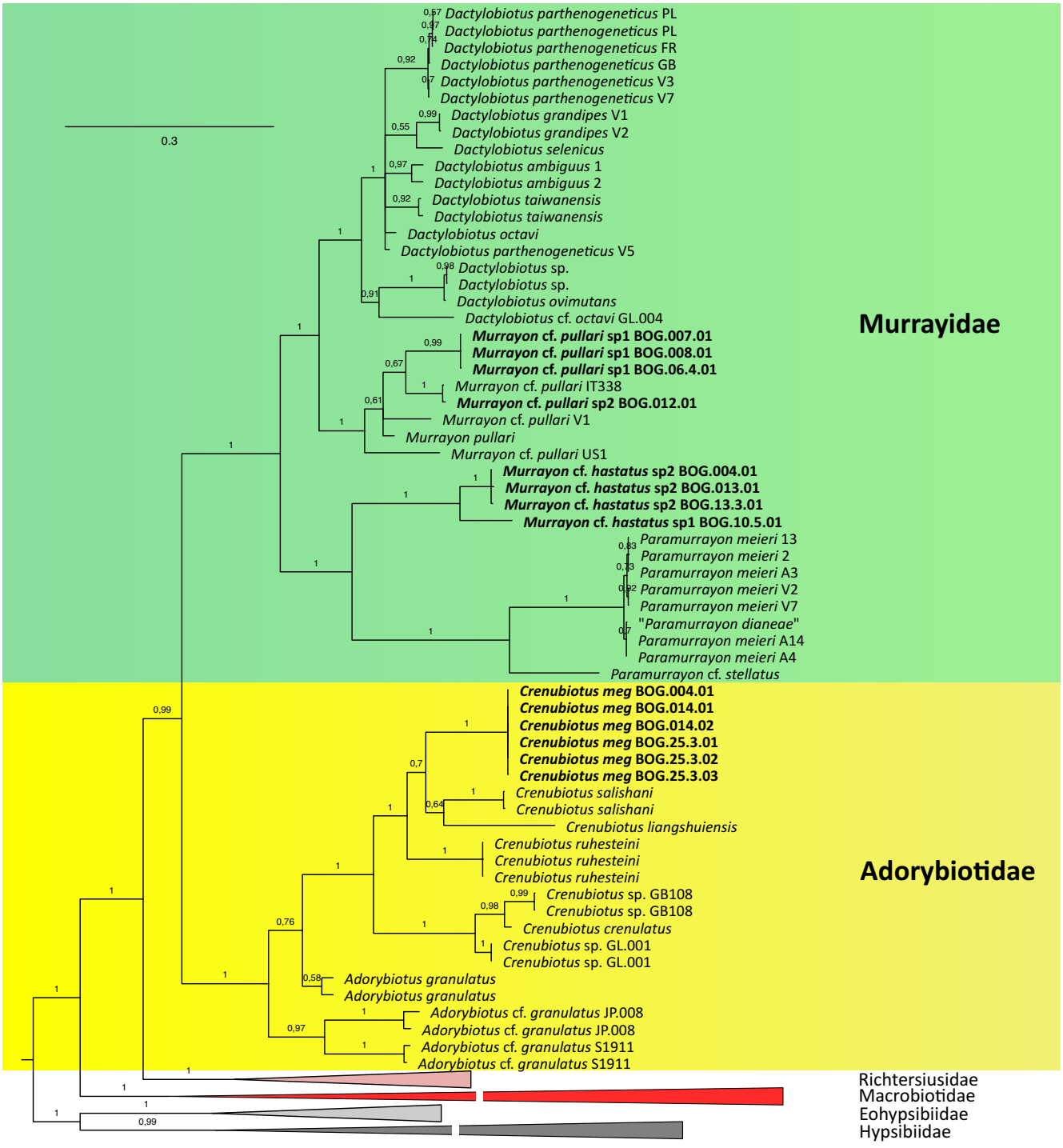

Fig. 1. Bayesian phylogenetic reconstruction of the superfamily Macrobiotoidea based on concatenated 18S rRNA + 28S rRNA + ITS-2 + COI nucleotide sequences. Values above branches indicate BI posterior probabilities (pp). Newly sequenced taxa/populations are bolded. Eohypsibidae and Hypsibiidae were used as outgroup. The scale bar represents substitutions per site.

Phylum: Tardigrada Doyère, 1840
Class: Eutardigrada Richters, 1926
Order: Parachela Schuster, Nelson, Grigarick & Christenberry, 1980
Superfamily: Macrobiotoidea Thulin, 1928
Family: Adorybiotidae Stec, Vecchi & Michalczyk 2020
Genus: *Crenubiotus* Lisi, Londoño & Quiroga, 2020

Crenubiotus meg **sp. nov.** Camarda, Fontaneto & Stec
ZooBank: urn:lsid:zoobank.org:act:5677D037-981C-4FB7-A0E1-A1BA7B37A2B6
(Tabs. 3 and 4; Figs. 2-8)

Etymology: The species epithet "*meg*" is treated as a noun in apposition and refers to the Molecular Ecology Group (MEG) at CNR-IRSA, Verbania (Italy). The name honours the open and collaborative research environment that enabled the study of this species.
Material examined: 72 animals, and 16 eggs. Specimens mounted on microscope slides in Hoyer's medium (62 animals + 14 eggs), fixed on SEM stubs (8 + 2), processed for DNA sequencing (2 animals).
Type locality: WGS84: 46.194365, 8.463157; 1868 m asl: Italy, Piedmont, Valle Vigezzo - Alpe i Motti; moss from an alpine fen; *Sphagnum fallax* (H.Klinggr.) H.Klinggr.; coll. 30.09.2024 by Daniel Bajorek and Diego Fontaneto.
Type depositories: Holotype (slide BOG.25.3.9 with 10 paratypes) and remaining 41 paratypes (slides: BOG.25.3.*, where the asterisk can be substituted by any of the following numbers 3-7) and 7 eggs (slide: BOG.25.3.2) are deposited at the Institute of Systematics and Evolution of Animals, Polish Academy of Sciences, Kraków, Poland; 10 paratypes (slide: BOG.25.3.8) and 7 eggs (slide: BOG.25.3.1) as well as SEM stub 105 with 8 paratypes and 2 eggs are deposited in the Pilato and Binda collection at the University of Catania, Italy.

Description of the new species

Animals (measurements and statistics in Tab. 3): When alive, the body is almost transparent in juveniles and yellowish in adults; after fixation in Hoyer's medium, the body becomes transparent (Fig. 2A). Eyes are present and remain visible in all specimens mounted in Hoyer's medium. The body cuticle bears circular to polygonal pores (0.2–1.2 µm in diameter), randomly distributed over the entire body cuticle, with the largest pores occurring in the dorso-cephalic and dorso-caudal regions (Figs. 2D and 3). Two large pores are present on the dorsal cuticle of the cephalic region near the mouth opening (Fig. 2 C-D). Distinct patches of dense, conspicuous granulation, composed of small tubercles or cushions with aggregations of microgranules on their surfaces, are present on all legs and on the dorso-caudal cuticle (Figs. 4 and 5). On legs I–III, the dense granulation forms two patches on the external and internal leg surfaces, respectively, which are connected by a narrower band of granulation extending proximally between the claws (Figs. 4 and 5). The external and internal patches on legs I–III coincide with two well-defined cuticular folds present on both sides of each leg (Figs. 4 and 5). In the proximal part of legs II and III, less developed fine granulation is also present on the frontal leg surface, connecting the external and internal patches, whereas such granulation is absent on leg I (Fig. 5 E,H). On leg IV, dense granulation evenly covers the dorsal and lateral surfaces (Fig. 3 A-C). Dense granulation is also present as a broad transverse band on the caudal cuticle, extending across the terminal body segment from the left lateral side, through the dorsal surface, to the right lateral side (Fig. 3 A-C). In addition to these dense granulation patches, very fine granulation is evenly distributed over the entire body surface but is visible only under SEM (Fig. 3D).
Claws slender, of the Richtersiidae type. Primary branches bear distinct accessory points and a long common tract with a system of internal septa; an evident stalk connects each claw to the lunula (Fig. 6). The common tract is apparently longer than half of the total claw height (Fig. 6). Large, comb-like, triangular lunulae with long, evenly distributed teeth are present on all legs (Fig. 6). Faint, divided cuticular bars (visible only in PCM) and paired muscle attachment sites are present just above the lunulae on legs I–III (Figs. 4D and 6 C,F,I).
Mouth antero-ventral. Bucco-pharyngeal apparatus of the modified *Macrobiotus* type (Fig. 7A), with ten peribuccal lamellae and a rigid buccal tube bearing a ventral lamina provided with an additional ventral thickening in its anterior portion. Based on LCM observations, the oral cavity armature appears poorly developed and composed exclusively of the second and third band of teeth (Fig. 7 B,C). The first band of teeth is visible only under SEM and is composed of few rows of granular teeth positioned at the base of peribuccal lamellae (Fig. 7D). The second band of teeth is situated between the ring fold and the third band and is composed of several rows of small cones, larger than those of the first band which under LCM are faintly seen as rough, granular band (Fig. 7C). The teeth of the third band are located in the posterior portion of the oral cavity, immediately anterior to the buccal tube opening (Fig. 7 B-D). This band is divided into dorsal and ventral portions. Under LCM, the dorsal portion appears as two distinct transverse ridges, each forming a globular thickening at the medial extremity; an obvious roundish median tooth is positioned anteriorly relative to the lateral teeth (Fig. 7D). The ventral portion consists of two lateral teeth that under LCM are seen as curved ridges, between which a roundish median tooth is present (Fig. 7B). The pharyngeal bulb is spherical, with triangular apophyses, three anterior cuticular spikes (typically only two visible in a single focal plane), two rod-shaped macroplacoids arranged with sequence 2<1, and a microplacoid positioned close to the second macroplacoid (Fig. 7E). The first macroplacoid is anteriorly narrowed and gently constricted medially, whereas the second macroplacoid exhibits a subterminal constriction (Fig. 7E).

Eggs (measurements and statistics in Tab. 4): Laid freely, whitish, spherical, bearing conical processes with elongated apices; the egg surface between processes lacks true areolation (Fig. 8). The elongated apices of the processes are sometimes multifurcated into short, flexible filaments or nodular projections (Fig. 8 A,B,G,H). Under LCM, the labyrinthine layer between the process walls is visible as a very faint reticular pattern with circular outlines (Fig. 8 A,B). This faint mesh is observable both in the proximal, wider portion of the processes and in part of their distal elongated portions (Fig. 8 A,B). Under SEM, the surface of the proximal, widened portion of the egg processes appears smooth, whereas the distal elongated portion is rough and covered with fine granulation (Fig. 8 H,I). The bases of the egg processes usually bear six finger-like projections, giving them a hexagonal outline when viewed from above (Fig. 8 A,B,H). Some of these projections may appear elongated into thin filaments under LCM; under SEM, these structures are visible as localized thickenings (Fig. 8 A,H). The finger-like projections often give the impression of near-complete connections between neighbouring processes, thereby forming a pattern of semi-areolation with six semi-areoles surrounding each process. The surface of the eggshell between processes appears smooth under LCM, but SEM reveals it to be distinctly wrinkled, with wrinkles oriented perpendicular to the egg processes (Fig. 8H).

Tab. 3. Measurements (in µm) of selected morphological structures of individuals from the type population of *Crenubiotus meg* sp. nov. mounted in Hoyer's medium.

Character	n	Range		Mean		SD		Holotype	
		µm	*pt*	µm	*pt*	µm	*pt*	µm	*pt*
Body length	20	187–431	*764–1163*	298	*969*	69	*110*	352	*1060*
Buccal tube									
Buccal tube length	20	23.2–37.0	–	30.4	–	4.2	–	33.2	–
Stylet support insertion point	20	16.9–27.7	*71.8–75.3*	22.4	*73.6*	3.1	*1.0*	24.2	*73.0*
Buccal tube external width	20	2.5–4.1	*9.9–12.5*	3.4	*11.2*	0.4	*0.5*	3.6	*10.9*
Buccal tube internal width	20	1.4–2.4	*5.8–7.6*	2.0	*6.5*	0.3	*0.5*	2.1	*6.2*
Ventral lamina length	16	11.6–20.5	*49.3–55.4*	15.7	*51.9*	2.5	*1.8*	16.4	*49.3*
Placoid lengths									
Macroplacoid 1	20	4.6–9.1	*18.1–26.0*	6.9	*22.6*	1.4	*2.1*	7.6	*22.8*
Macroplacoid 2	20	3.2–6.7	*13.5–20.2*	5.1	*16.6*	1.1	*1.7*	6.6	*19.9*
Microplacoid	20	1.1–2.8	*4.7–7.6*	1.9	*6.3*	0.4	*0.8*	2.1	*6.4*
Macroplacoid row	20	8.9–16.6	*37.3–49.8*	13.3	*43.4*	2.5	*3.1*	15.4	*46.4*
Placoid row	20	10.4–19.5	*43.5–55.7*	15.7	*51.2*	2.8	*3.2*	17.2	*51.8*
Claw I heights									
External base	11	3.3–6.0	*13.1–16.5*	4.5	*14.5*	0.7	*1.0*	4.4	*13.1*
External primary branch	17	4.9–9.3	*20.6–25.2*	7.1	*23.3*	1.2	*1.3*	7.5	*22.6*
External secondary branch	17	3.8–7.6	*16.0–20.7*	5.8	*19.2*	1.0	*1.2*	6.2	*18.8*
External base/primary branch (*cct*)	11	*55.7–67.3*	–	*62.2*	–	*3.7*	–	*58.1*	–
Internal base	9	2.8–4.9	*11.6–14.8*	4.0	*13.3*	0.8	*1.1*	4.6	*14.0*
Internal primary branch	17	4.5–8.9	*18.8–24.8*	6.9	*22.7*	1.3	*1.5*	7.5	*22.6*
Internal secondary branch	17	3.8–7.5	*15.7–21.0*	5.7	*18.8*	1.1	*1.4*	5.9	*17.8*
Internal base/primary branch (*cct*)	9	*56.7–62.4*	–	*59.6*	–	*2.1*	–	*61.8*	–
Claw II heights									
External base	13	2.9–5.2	*12.3–16.8*	4.3	*14.4*	0.7	*1.5*	4.8	*14.3*
External primary branch	17	5.0–9.2	*20.8–25.9*	7.2	*23.9*	1.3	*1.6*	7.7	*23.1*
External secondary branch	18	4.2–7.3	*17.4–21.9*	6.0	*19.9*	1.0	*1.4*	6.6	*19.7*
External base/primary branch (*cct*)	13	*50.2–67.9*	–	*61.1*	–	*4.4*	–	*62.1*	–
Internal base	14	2.8–5.2	*11.6–15.8*	4.2	*13.9*	0.8	*1.3*	4.8	*14.6*
Internal primary branch	17	4.7–8.8	*19.4–24.6*	6.8	*22.5*	1.3	*1.5*	7.7	*23.1*
Internal secondary branch	17	3.8–7.7	*16.0–20.8*	5.7	*18.9*	1.1	*1.3*	6.3	*18.8*
Internal base/primary branch (*cct*)	14	*56.5–70.0*	–	*63.0*	–	*5.1*	–	*63.1*	–
Claw III heights									
External base	10	3.6–4.9	*13.2–15.4*	4.4	*14.4*	0.4	*0.9*	?	?
External primary branch	15	5.5–9.5	*20.7–25.9*	7.4	*24.3*	1.2	*1.4*	?	?
External secondary branch	16	4.5–8.0	*17.4–22.6*	6.1	*20.2*	1.0	*1.4*	?	?
External base/primary branch (*cct*)	10	*53.8–64.1*	–	*59.9*	–	*3.2*	–	?	–
Internal base	10	3.2–5.4	*11.7–16.0*	4.4	*13.7*	0.7	*1.3*	?	?
Internal primary branch	15	5.2–9.1	*19.8–24.6*	6.8	*22.5*	1.2	*1.3*	?	?
Internal secondary branch	15	4.1–7.7	*16.8–20.7*	5.7	*18.8*	1.1	*1.3*	?	?
Internal base/primary branch (*cct*)	10	*56.4–69.4*	–	*60.2*	–	*3.9*	–	?	–
Claw IV heights									
Anterior base	15	3.2–5.8	*13.6–17.0*	4.5	*15.0*	0.8	*1.0*	5.1	*15.2*
Anterior primary branch	19	5.0–10.2	*21.6–27.6*	7.4	*24.5*	1.4	*1.9*	8.1	*24.4*
Anterior secondary branch	19	4.1–8.0	*17.5–22.0*	6.0	*19.8*	1.2	*1.6*	6.9	*20.7*
Anterior base/primary branch (*cct*)	15	*55.9–66.7*	–	*62.2*	–	*3.7*	–	*62.4*	–
Posterior base	13	3.3–5.8	*14.2–16.3*	4.6	*15.3*	0.7	*0.7*	?	?
Posterior primary branch	20	5.5–9.9	*21.8–26.8*	7.6	*25.0*	1.3	*1.5*	8.6	*25.8*
Posterior secondary branch	19	4.4–8.1	*17.8–22.4*	6.1	*20.1*	1.1	*1.5*	?	?
Posterior base/primary branch (*cct*)	13	*59.1–71.2*	–	*62.1*	–	*3.3*	–	?	–

n, number of specimens/structures measured; Range, refers to the smallest and the largest structure among all measured specimens; SD, standard deviation.

Tab. 4. Measurements (in µm) of selected morphological structures of the eggs from the type population *Crenubiotus meg* sp. nov. mounted in Hoyer's medium.

Character	n	Range	Mean	SD
Egg bare diameter	14	52.5–70.8	64.3	4.6
Egg full diameter	14	93.0–108.6	100.5	4.4
Process height	42	14.7–23.0	17.7	2.0
Process base width	42	11.7–20.0	15.4	1.6
Process base/height ratio	42	59%–109%	88%	13%
Inter-process distance	42	2.6–7.2	4.4	1.1
Number of processes on the egg circumference	14	11–13	12.0	0.7

n, number of eggs/structures measured; Range, refers to the smallest and the largest structure among all measured specimens; SD, standard deviation.

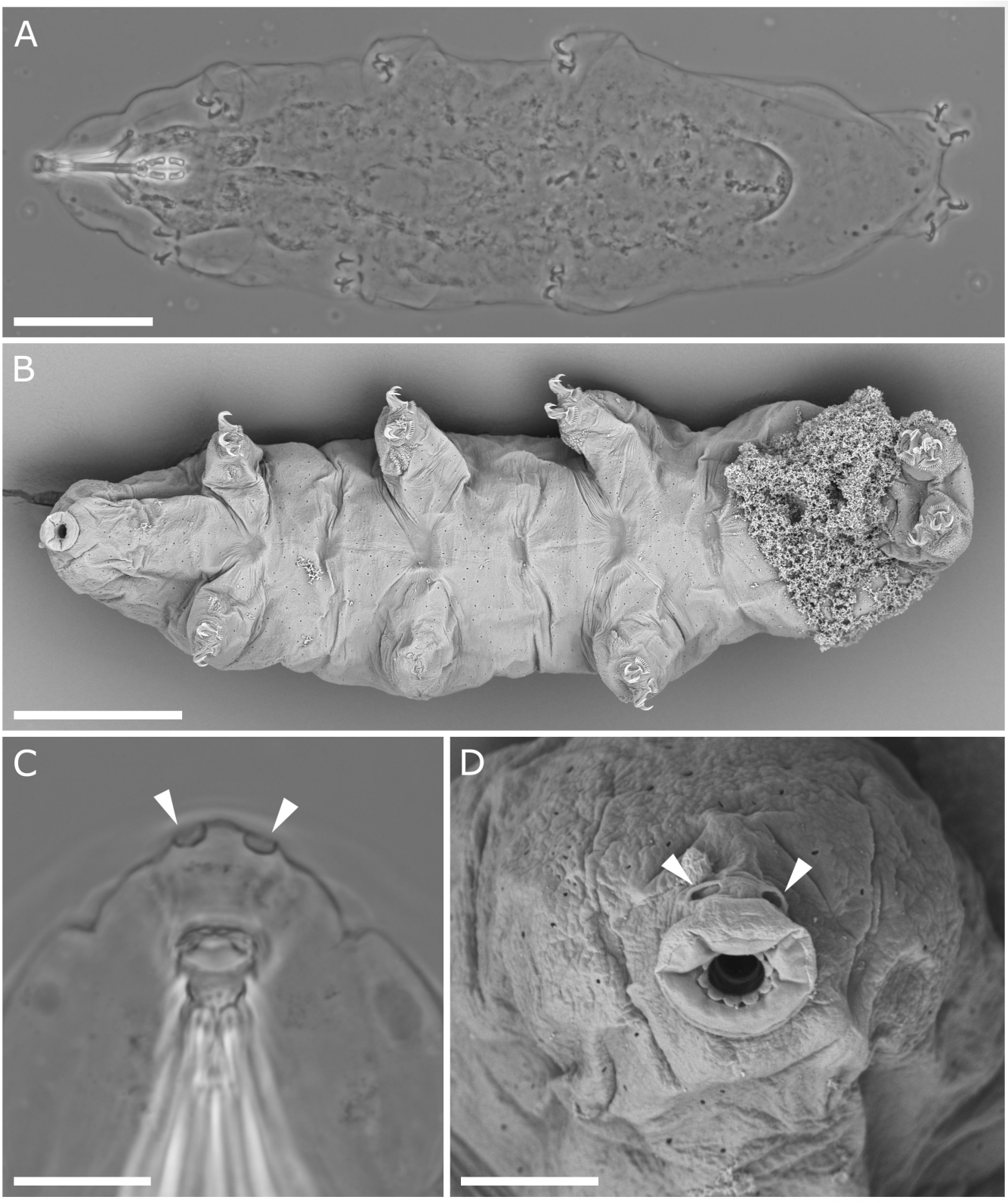

Fig. 2. *Crenubiotus meg* sp. nov., habitus and large dorsal pores near the mouth opening. (**A**) Habitus observed in PCM (holotype). (**B**) Habitus observed in SEM (paratype). (**C–D**) Two large pores in the dorsal cuticle of the cephalic region near the mouth opening, shown in PCM and SEM, respectively (both paratypes). Filled flat arrowheads indicate the two large pores. Scale bars: A,B) 50 µm; C,D) 10 µm.

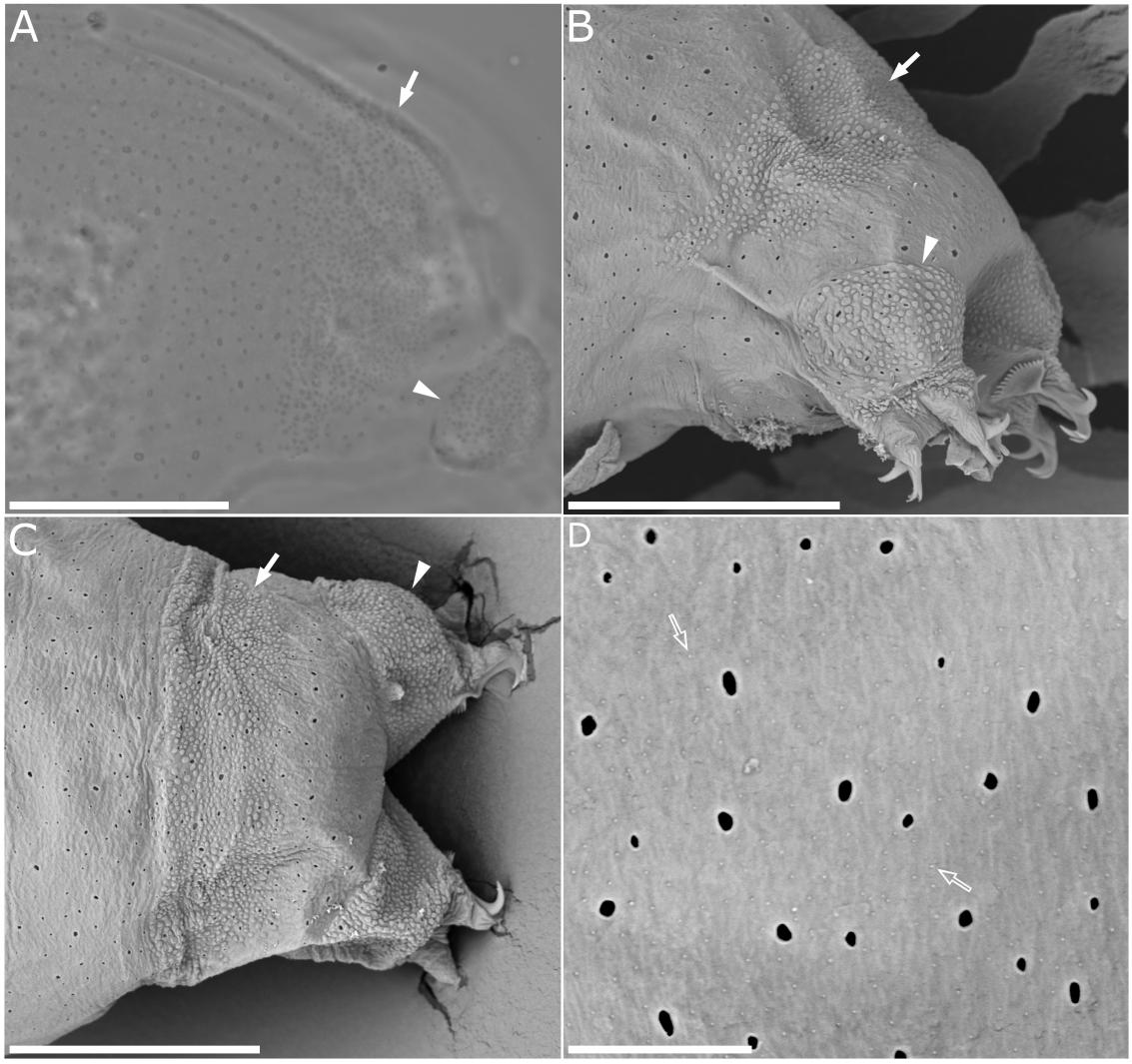

Fig. 3. *Crenubiotus meg* sp. nov., cuticular morphology in the caudal body region. (**A**) Pores, caudal band of dense granulation, and granulation on the hind legs observed in PCM (holotype/paratype). (**B–C**) Pores, caudal band of dense granulation, and granulation on the hind legs observed in SEM, shown in lateral and dorso-ventral views, respectively (paratypes). (**D**) Dorso-lateral cuticle showing pores and a very fine granulation (paratype). Filled arrows indicate the caudal band of dense granulation; empty arrows indicate fine, delicate granulation covering the entire body cuticle; filled flat arrowheads indicate dense granulation on the hind legs. Scale bars: A-C) 30 µm; D) 5 µm.

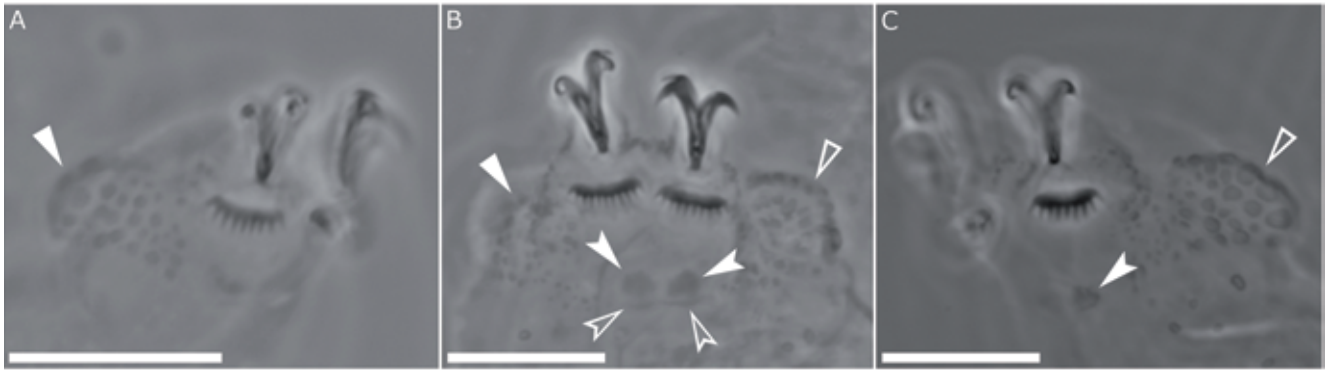

Fig. 4. *Crenubiotus meg* sp. nov., cuticular morphology of the legs observed in PCM (all paratypes). (**A**) Patch of dense granulation on the external surface of leg II. (**B**) Posterior surface of leg II. (**C**) Patch of dense granulation on the internal surface of leg II. Filled flat arrowheads indicate the cuticular fold and dense granulation on the external leg surface; empty flat arrowheads indicate the cuticular fold and dense granulation on the internal leg surface; filled indented arrowheads indicate divided cuticular bars; empty indented arrowheads indicate muscle attachment sites. Scale bar: 10 µm.

Reproductive mode

The examination of 62 animals freshly mounted in Hoyer's medium revealed no testes or spermathecae filled with spermatozoa, which suggests that the species is (at least facultatively) parthenogenetic.

DNA sequences

We obtained sequences for all four of the above-mentioned molecular markers from two individuals of the type population destined for DNA extraction and sequencing, which are as follow: PX698796 and PX698797 (18S rRNA), PX698818 and PX698818 (28S rRNA), PX698835 and PX698836 (ITS-2), PX701242 and PX701246 (COI).

Remarks

The new species seems to be quite common in the studied region as it was found in 10 out of 35 samples analysed in this study (BOG.004, BOG.008, BOG.012, BOG.014, BOG.015, BOG.13.3, BOG.14.5, BOG.15.2, BOG.23.2, BOG.25.3) with populations from BOG.004 and BOG.014 being also genetically verified (Supplementary Materials SM.04 and SM.05).

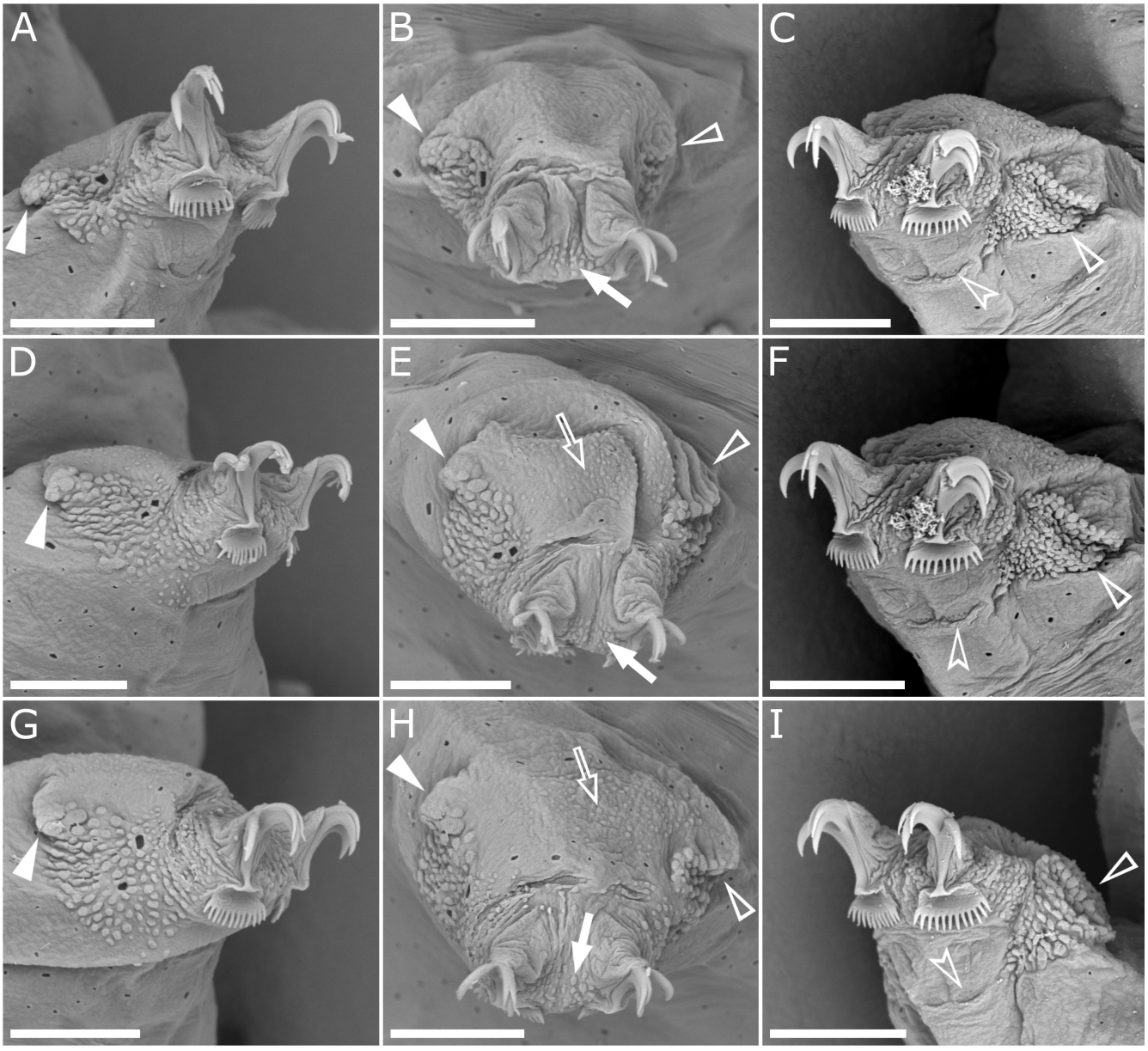

Fig. 5. *Crenubiotus meg* sp. nov., cuticular morphology of the legs observed in SEM. (**A,D,G**) External surface of legs I, II, and III, respectively (paratypes). (**B,E,H**) Frontal surface of legs I, II, and III, respectively (paratype). (**C,F,I**) Internal surface of legs I, II, and III, respectively (paratypes). Filled flat arrowheads indicate the cuticular fold and dense granulation on the external leg surface; empty flat arrowheads indicate the cuticular fold and dense granulation on the internal leg surface; filled arrows indicate a narrower band of granulation extending proximally between the claws; empty arrows indicate less developed fine granulation on the frontal leg surface; empty indented arrowheads indicate muscle attachment sites. Scale bar: 10 µm.

Differential diagnosis

To date, the genus *Crenubiotus* comprises five nominal species: *Cre. crenulatus*, *Crenubiotus liangshuiensis* J.-Y. Zhang, X.-L. Sun, N. Wang, Hao, Ma, N. Zhao, H. Li, M. Zhao & S.-T. Yang, 2024, *Crenubiotus revelator* Lisi, Londoño & Quiroga, 2020, *Crenubiotus ruhesteini* Guidetti, Schill, Giovannini, Massa, Goldoni, Ebel, Förschler, Rebecchi & Cesari, 2021, and *Crenubiotus salishani* Vecchi, Choong & Calhim, 2022. The new species differs markedly from all congeners in egg morphology. Specifically, it possesses well-developed, six finger-like projections at the bases of the egg processes giving it hexagonal-shape, which frequently form a pattern of semi-areolation with six semi-areoles surrounding each process. In contrast, all other known *Crenubiotus* species lack this character and exhibit egg processes with circular or weakly lobed bases without distinct finger-like projections.

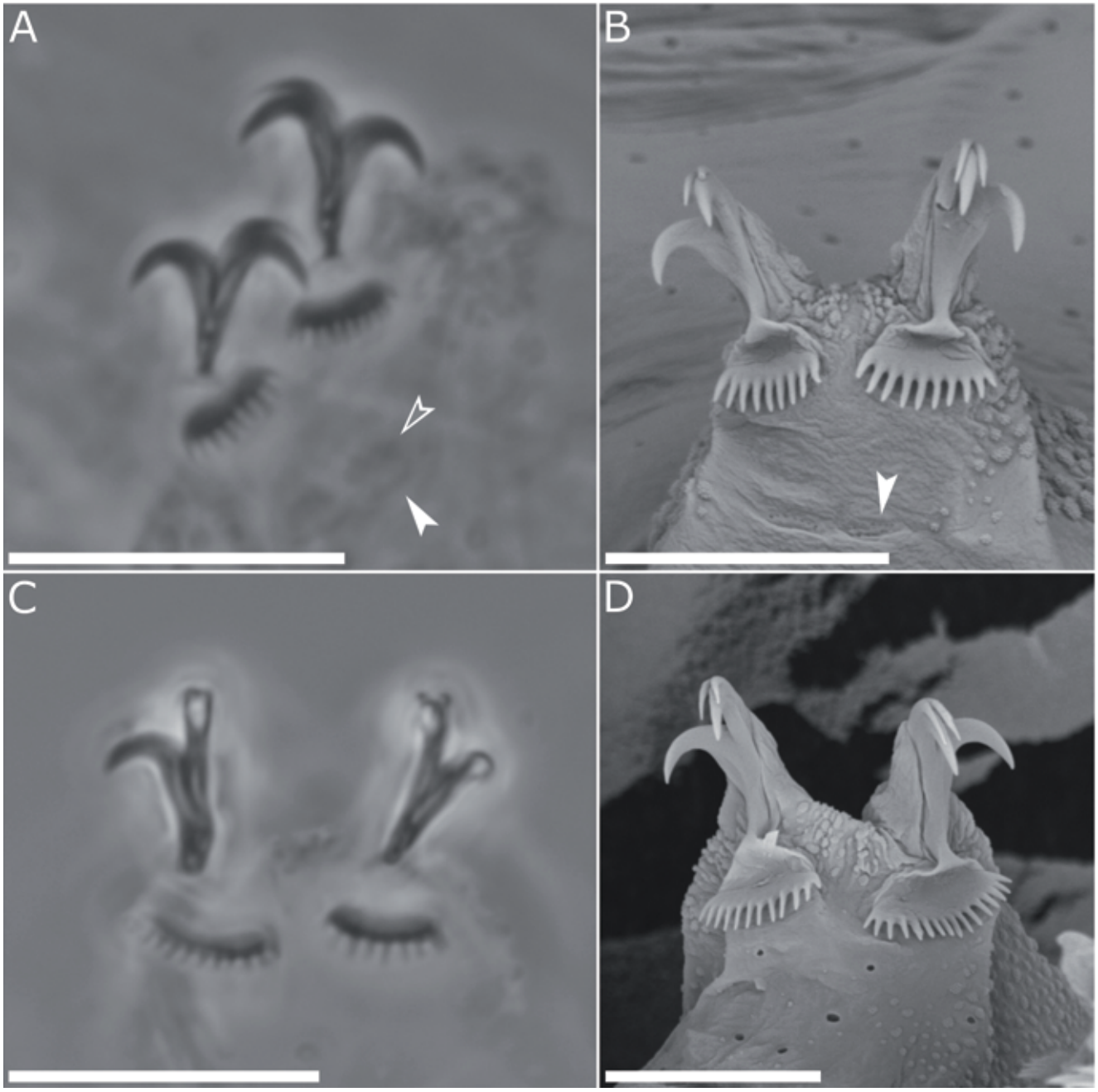

Fig. 6. *Crenubiotus meg* sp. nov., claw morphology. (**A**) Claws II observed in PCM (paratype). (**B**) Claws II observed in SEM (paratype). (**C**) Claws IV observed in PCM (paratype). (**D**) Claws IV observed in SEM (paratype). Scale bar: 10 μm.

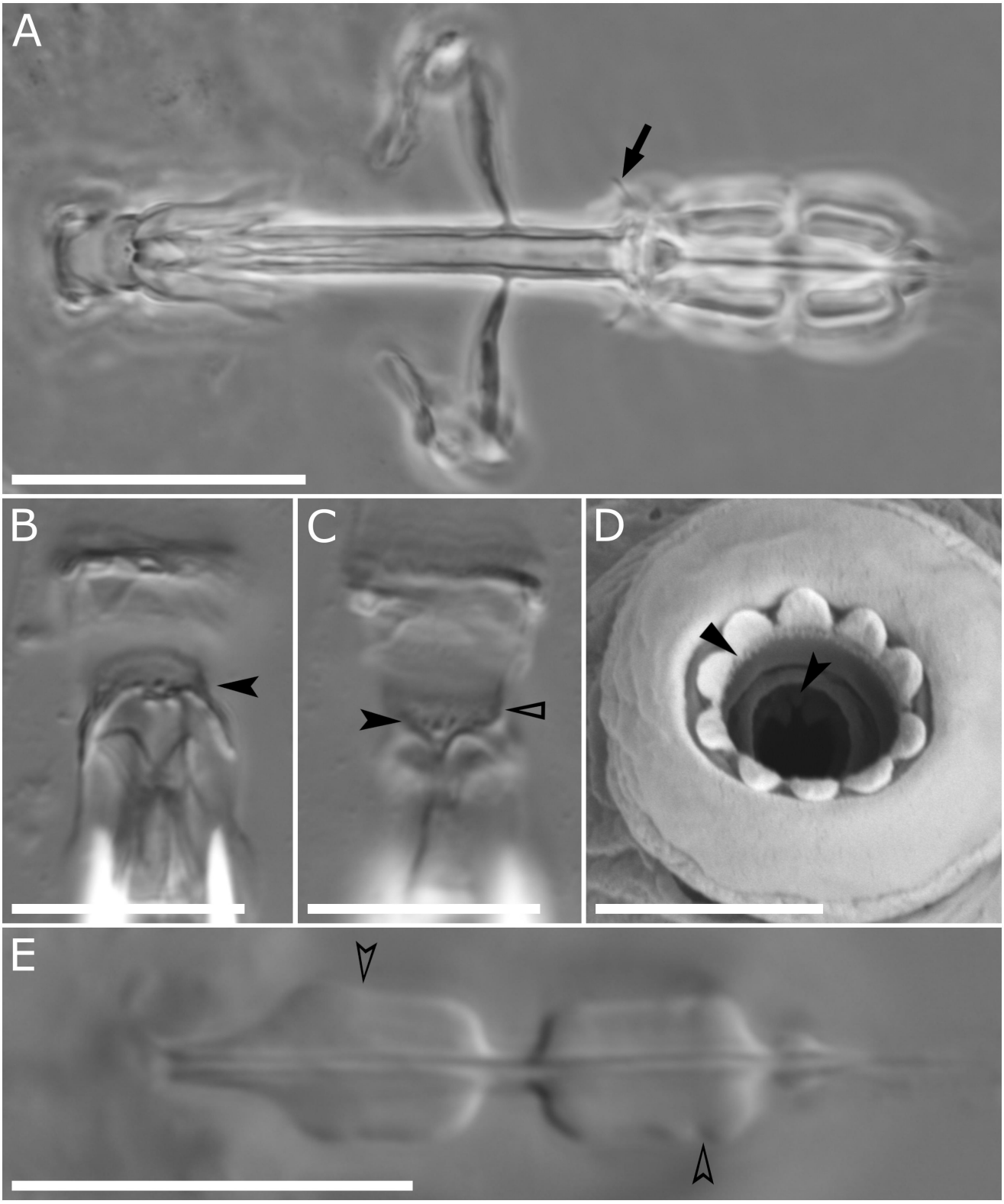

Fig. 7. *Crenubiotus meg* sp. nov., morphology of the bucco-pharyngeal apparatus and oral cavity armature. (**A**) Dorsal view of the entire bucco-pharyngeal apparatus observed in PCM (paratype). (**B**) Dorsal view of the oral cavity armature (OCA) observed in DIC (paratype). (**C**) Ventral view of the OCA observed in DIC (paratype). (**D**) Dorsal view of the OCA observed in SEM (paratype). (**E**) Placoid configuration observed in DIC (Holotype). Filled flat arrowheads indicate the first band of teeth; empty flat arrowheads indicate the second band of teeth; filled indented arrowheads indicate the third band of teeth; empty indented arrowheads indicate constrictions in the macroplacoids; arrows indicate lateral spikes. Scale bars: A) 20 µm; B,C,E) 10 µm; D) 5 µm.

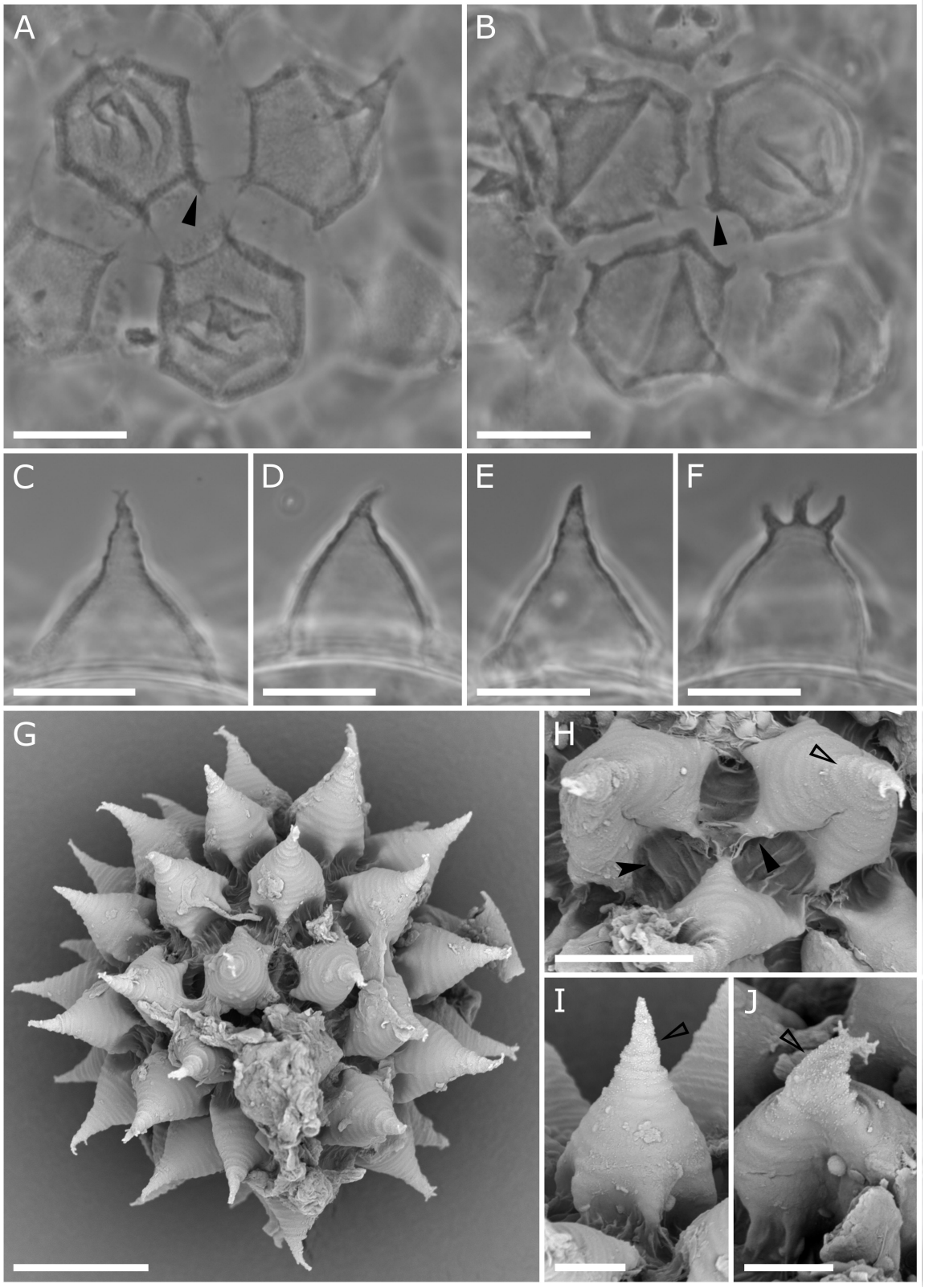

Fig. 8. *Crenubiotus meg* sp. nov., egg morphology. (**A,B**) Details of the egg shell and egg process surface observed in PCM. (**C-F**) Midsections of egg processes. (**G**) Entire egg observed in SEM. (**H-J**) Details of egg processes and egg shell surface observed in SEM. Filled flat arrowheads indicate large finger-like projections at the bases of egg processes; empty flat arrowheads indicate granulation on the distal portions of egg processes; filled indented arrowheads indicate wrinkles within the semi-areolae. Scale bars: A-F,H) 10 µm; G) 20 µm; I,J) 5 µm.

In addition, the new species is distinguished by the configuration of the oral cavity armature observed under light contrast microscopy (LCM). In the new species, the dorsal portion of the oral cavity armature consists of two distinct transverse ridges, each forming a globular thickening at the medial extremity, and bears a conspicuous, roundish median tooth positioned anteriorly relative to the lateral teeth. The ventral portion comprises two lateral teeth visible as curved ridges, between which a distinct, roundish median tooth is present. In contrast, *Cre. crenulatus*, *Cre. liangshuiensis*, and *Cre. ruhesteini* lack median teeth in both the dorsal and ventral portions of the oral cavity, which in these species are composed solely of transverse ridges without distinct median elements. *Cre. revelator* possesses a median tooth only in the ventral portion, whereas the dorsal portion lacks such a structure. Finally, *Cre. salishani* shows a single median tooth located anterior to the dorsal ridges in the dorsal portion of the third band of teeth, while a median tooth is absent in the ventral portion.

Superfamily: Hypsibioidea Pilato, 1969
Family: Pilatobiidae Bertolani, Guidetti, Marchioro, Altiero, Rebecchi & Cesari, 2014
Genus: *Fontourion* Gąsiorek, Morek & Michalczyk, 2024

Fontourion secchii (Bertolani & Rebecchi, 1996)
(Tab. 5; Figs. 9-11)
Material examined: 83 animals. Specimens mounted on microscope slides in Hoyer's medium (77 animals), fixed on SEM stubs (4), processed for DNA sequencing (2).

Tab. 5. Measurements (in µm) of selected morphological structures of individuals of *Fontourion secchii* (Bertolani & Rebecchi, 1996) from Italy mounted in Hoyer's medium.

Character	n	Range		Mean		SD	
		µm	*pt*	µm	*pt*	µm	*pt*
Body length	19	219–402	*1140–1715*	317	*1412*	52	*175*
Buccopharyngeal tube							
Buccal tube length	20	18.6–28.8	–	22.5	–	2.5	–
Pharyngeal tube length	20	39.4–56.0	*143.0–230.0*	45.3	*202.5*	4.0	*19.3*
Buccopharyngeal tube length	20	59.2–80.4	*243.0–330.1*	67.8	*302.4*	5.4	*19.2*
Buccal/pharyngeal tube length ratio	20	43%–70%	–	50%	–	6%	–
Stylet support insertion point	18	12.9–16.5	*64.3–70.1*	14.9	*66.8*	1.1	*1.7*
Buccal tube external width	19	1.6–2.2	*7.2–9.8*	1.9	*8.6*	0.2	*0.8*
Buccal tube internal width	19	0.8–1.1	*3.6–4.9*	0.9	*4.1*	0.1	*0.3*
Placoid lengths							
Macroplacoid 1	20	5.3–8.6	*25.8–34.7*	6.7	*29.5*	0.9	*2.2*
Macroplacoid 2	20	3.7–6.4	*18.7*–0.9	*2.4*			
Septulum	19	2.0–2.8	*7.5–13.3*	2.4	*10.7*	0.3	*1.1*
Macroplacoid row	20	10.0–16.1	*50.5–64.6*	12.7	*56.4*	1.8	*4.2*
Placoid row	19	12.8–20.0	*61.3–80.2*	16.1	*71.5*	2.2	*5.4*
Claw I heights							
External base	18	4.1–6.0	*19.2–26.6*	4.9	*22.0*	0.6	*1.9*
External primary branch	17	7.9–11.4	*35.9–6.8*	9.6	*43.1*	1.1	*3.1*
External secondary branch	16	4.6–7.8	*24.2–32.2*	6.4	*28.9*	0.9	*2.3*
Internal base	11	3.6–5.3	*17.3–20.9*	4.4	*19.3*	0.5	*1.1*
Internal primary branch	11	5.2–7.1	*24.6–29.9*	6.2	*27.5*	0.6	*1.6*
Internal secondary branch	7	3.6–4.8	*16.4–21.9*	4.3	*18.9*	0.4	*1.9*
Claw II heights							
External base	17	4.5–6.7	*18.4–28.5*	5.5	*24.6*	0.6	*2.7*
External primary branch	15	8.7–13.4	*45.5–57.6*	10.9	*49.6*	1.5	*3.4*
External secondary branch	15	4.9–9.1	*17.0–36.7*	6.7	*30.0*	1.2	*4.6*
Internal base	14	3.9–5.8	*17.3–23.4*	4.8	*21.4*	0.7	*1.8*
Internal primary branch	16	5.9–8.9	*24.9–37.9*	7.3	*32.3*	0.8	*3.2*
Internal secondary branch	14	4.0–6.7	*13.8–27.4*	5.1	*22.5*	0.8	*3.5*
Claw III heights							
External base	18	4.4–6.7	*21.2–30.3*	5.7	*25.6*	0.7	*2.3*
External primary branch	14	7.6–12.3	*33.6–56.1*	10.4	*47.7*	1.3	*6.4*
External secondary branch	17	5.2–8.6	*18.9–37.5*	6.9	*30.6*	1.0	*4.3*
Internal base	15	4.1–5.9	*19.7–25.0*	5.0	*22.2*	0.6	*1.5*
Internal primary branch	16	5.9–8.6	*23.7–37.6*	7.3	*32.2*	0.9	*4.0*
Internal secondary branch	15	4.3–6.8	*15.8–28.2*	5.5	*24.5*	0.8	*3.3*
Claw IV heights							
Anterior base	19	3.6–6.1	*14.0–25.9*	4.7	*21.1*	0.7	*2.7*
Anterior primary branch	19	6.1–9.1	*23.5–36.6*	7.3	*32.8*	0.9	*3.0*
Anterior secondary branch	17	4.0–6.9	*17.9–31.6*	5.5	*24.4*	0.8	*3.8*
Posterior base	20	4.6–7.7	*22.7–32.9*	6.2	*27.7*	1.0	*2.9*
Posterior primary branch	19	10.3–14.9	*42.4–64.0*	12.3	*55.0*	1.3	*4.6*
Posterior secondary branch	18	5.6–8.5	*26.1–37.2*	7.2	*32.1*	0.9	*2.6*

n, number of specimens/structures measured; Range, refers to the smallest and the largest structure among all measured specimens; SD, standard deviation.

Locality: WGS84: 46.15697, 8.170665; 1832 m asl: Italy, Piedmont, Valle Bognanco, Torbiera di Gattascosa; moss from an alpine fen; *Sphagnum teres* (Schimp.) Ångstr.; coll. 28.10.2023 by Daniel Bajorek, Daniel Stec and Diego Fontaneto.
Specimen depositories: 77 animals mounted in slides BOG.002.*, where the asterisk can be substituted by any of the following numbers: 1-4 and 6-8) are deposited at the Institute of Systematics and Evolution of Animals, Polish Academy of Sciences, Kraków, Poland; SEM stub 106 with 4 animals is deposited in the Pilato and Binda collection at the University of Catania, Italy.

Description of the newly found population

Animals (measurements and statistics in Tab. 5): Body elongated, whitish, covered with smooth cuticle (Fig. 9).

Fig. 9. *Fontourion secchii* (Bertolani & Rebecchi, 1996) from Italy, habitus. (**A**) Habitus observed in PCM. (**B**) Habitus observed in SEM. Scale bar: 50 µm.

Dorsal cuticle wrinkled under SEM; however, this is probably a preparation artifact as wrinkles of that size should be well visible in LCM (Figs. 9 and 11 E,F). Eyes absent in specimens mounted in Hoyer's medium. Buccopharyngeal tube composed by a rigid buccal tube followed by a flexible annulated pharyngeal tube (Fig. 10A). Oral cavity armature not visible under LCM. Stylet furcae of the *Hypsibius* type. A prominent, dorsally placed, oval drop-like thickening on the border between the buccal and the pharyngeal tube present (Fig. 10A). Annulation regular, singular dorsally and ventrally, and net-like laterally (i.e., the pharyngeal annulation is semi-complex; annuli single laterally and forking dorsoventrally; Fig. 10A). A short, very posterior part of the pharyngeal tube without annulation (Fig. 10). Pharyngeal bulb with two macroplacoids and a septulum (Fig. 10 B,C). Macroplacoid length sequence 1>2; macroplacoids bar-shaped, arranged in parallel rows (Fig. 10 B,C). The first macroplacoid with a deep mid-constriction, in some specimens the constriction being so strong that the placoid may give the appearance of the presence of two distinct placoids (Fig. 10 B,C). The second macroplacoid with an evident subterminal constriction (Fig. 10). An obvious drop-shaped septulum present (Fig. 10B).
Claws of the *Hypsibius* type, with widened bases and with apparent accessory points on the primary branches (Figs. 10 D-F and 11 A-E). Internal and anterior claws with two clear septa dividing the claw into the basal portion, the secondary branch, and the primary branch (Fig. 10). External and posterior claws without septa (Fig. 10 D-F). The base of the external and posterior claws extends towards the base of the anterior claw, forming a small cuticular bar (Figs. 10 D-F and 11 A-E). Internal and anterior claws with pseudolunulae at their bases (Figs. 9 and 10). External and posterior claws without pseudolunulae but with an enlarged base provided with small cuticular bars protruding toward the pseudolunula of internal/anterior claw (Figs. 10 D-F and 11 A-E).

Eggs: Roundish and smooth, deposited in exuviae.

DNA sequences
We obtained sequences for all four of the above-mentioned molecular markers from two individuals of the newly found population destined for DNA extraction and sequencing, which are as follow: PX698788 and PX698787 (18S rRNA), PX698817 and PX698816 (28S rRNA), PX698834 and PX698833 (ITS-2), PX701231 and PX701232 (COI).

Remarks
This species was found in 7 of the 35 samples analysed in this study (BOG.001, BOG.002, BOG.003, BOG.004, BOG.014, BOG.015, BOG.06.4, BOG.07.1; Supplementary Materials SM.05). The *Fontourion* population examined here is genetically distinct from all other recognised congeners for which molecular data are available, with COI p-distances exceeding 17% when compared with *Fontourion glaciale* (Zawierucha, Buda & Gąsiorek, 2020), *Fontourion islandicum* (Buda & Zawierucha, 2018), and *Fontourion recamieri* (Richters, 1911) (Supplementary Materials SM.05). The examined material shows no consistent morphological differences from *Fontourion secchii*. A weak difference in macroplacoid length was tentatively noted when comparing our specimens with photomicrographs of the holotype (Supplementary Materials SM.06); however, published morphometric data for *Fon. secchii* types (Gąsiorek *et al.*, 2017) overlap with measurements obtained from the newly examined population. Given the geographic proximity to the type locality of *Fon. secchii* (Monte Rondinaio in the Tusco–Emilian Apennines, approximately 290 km from our sampling site), we assign our population to this species and regard *Fon. secchii* as a valid taxon based on its clear genetic separation from other sequenced *Fontourion* species.

Family: Microhypsibiidae Pilato, 1998
Genus: *Microhypsibius* Thulin, 1928

Microhypsibius minimus Kristensen, 1982
(Tab. 6; Figs. 12-14)
Material examined: 31 animals. Specimens mounted on microscope slides in Hoyer's medium (24 animals), fixed on SEM stubs (4), processed for DNA sequencing (3).
Locality: WGS84: 46.459701, 8.453291; 2312 m asl: Switzerland, Bedretto, Passo San Giacomo; moss from an alpine fen; *Climacium dendroides* (Hedw.) F. Weber & D. Mohr; coll. 25.09.2024 by Daniel Bajorek, Daniel Stec and Diego Fontaneto.
Specimen depositories: 24 animals mounted in slides BOG.06.4.*, where the asterisk can be substituted by any of the following numbers: 9-10 and 12-24) are deposited at the Institute of Systematics and Evolution of Animals, Polish Academy of Sciences, Kraków, Poland; SEM stub 110 with 2 animals is deposited in the Pilato and Binda collection at the University of Catania, Italy.

Description of the newly found population

Animals (measurements and statistics in Tab. 6): Body short, with the caudal portion slightly enlarged (Fig. 12 A,B), transparent both before and after mounting in Hoyer's medium. Cuticle smooth or slightly wrinkled under LCM; however, a delicate reticulation delineated by small depressions is visible under SEM (Fig. 12C). Eyes absent in specimens mounted in Hoyer's medium. Buccal tube rigid without ventral lamina (Fig. 13 A,B). Oral cavity armature absent or not visible under LCM. Apophyses for the insertion of the stylet muscles (AISM) asymmetrical with respect to the frontal plane of the rigid tube (Fig. 13 B-D); the ventral apophysis forms a longitudinal undulating crest, anteriorly and posteriorly thickened and with a more prominent and refractive medial portion under PCM, whereas the dorsal crest constitute an undulating thickened ridge, more prominent anteriorly and bearing a medial depression (Fig. 13 C,D). The pharyngeal bulb with three macroplacoids, a faint microplacoid, and a well-developed septulum (Fig. 13 E,F). Macroplacoid length sequence 3>2>1; macroplacoids bar-shaped and arranged in parallel rows (Fig. 13 E,F). The microplacoid is present, positioned closer to the septulum than to the third macroplacoid, and is sometimes difficult to observe (Fig. 13 B,E,F). A distinct drop-shaped septulum is present and always well visible (Fig. 13 A,B,E,F). Claws of the *Microhypsibius*-type, with internal septa separating the primary and secondary branches, and depending on the observation perspective giving the impression that either the primary branch is inserted on the secondary branch or the secondary branch is inserted on the primary branch (Fig. 14). Pseudolunulae and cuticular bars are absent or not visible (Fig. 14).

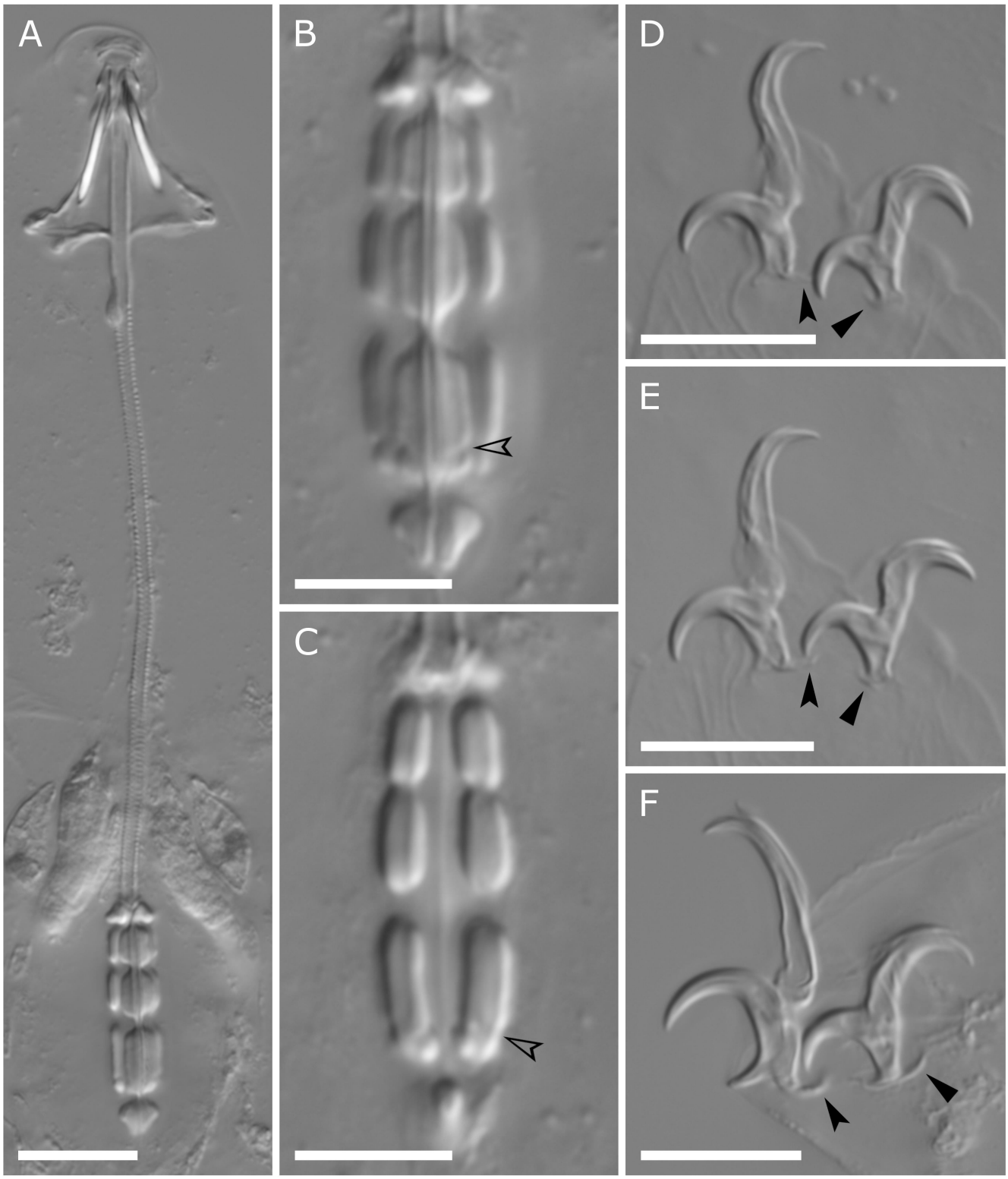

Fig. 10. *Fontourion secchii* (Bertolani & Rebecchi, 1996) from Italy, bucco-pharyngeal apparatus and claws observed in DIC. (**A**) Entire bucco-pharyngeal apparatus. (**B,C**) Placoids in ventral and dorsal view, respectively. (**D-F**) Claws II, III, and IV, respectively. Empty indented arrowheads indicate constrictions in the macroplacoids; filled flat arrowheads indicate pseudolunulae; filled indented arrowhead indicate the small cuticular bars. Scale bar: A,E-F) 10 µm: B,C) 5 µm.

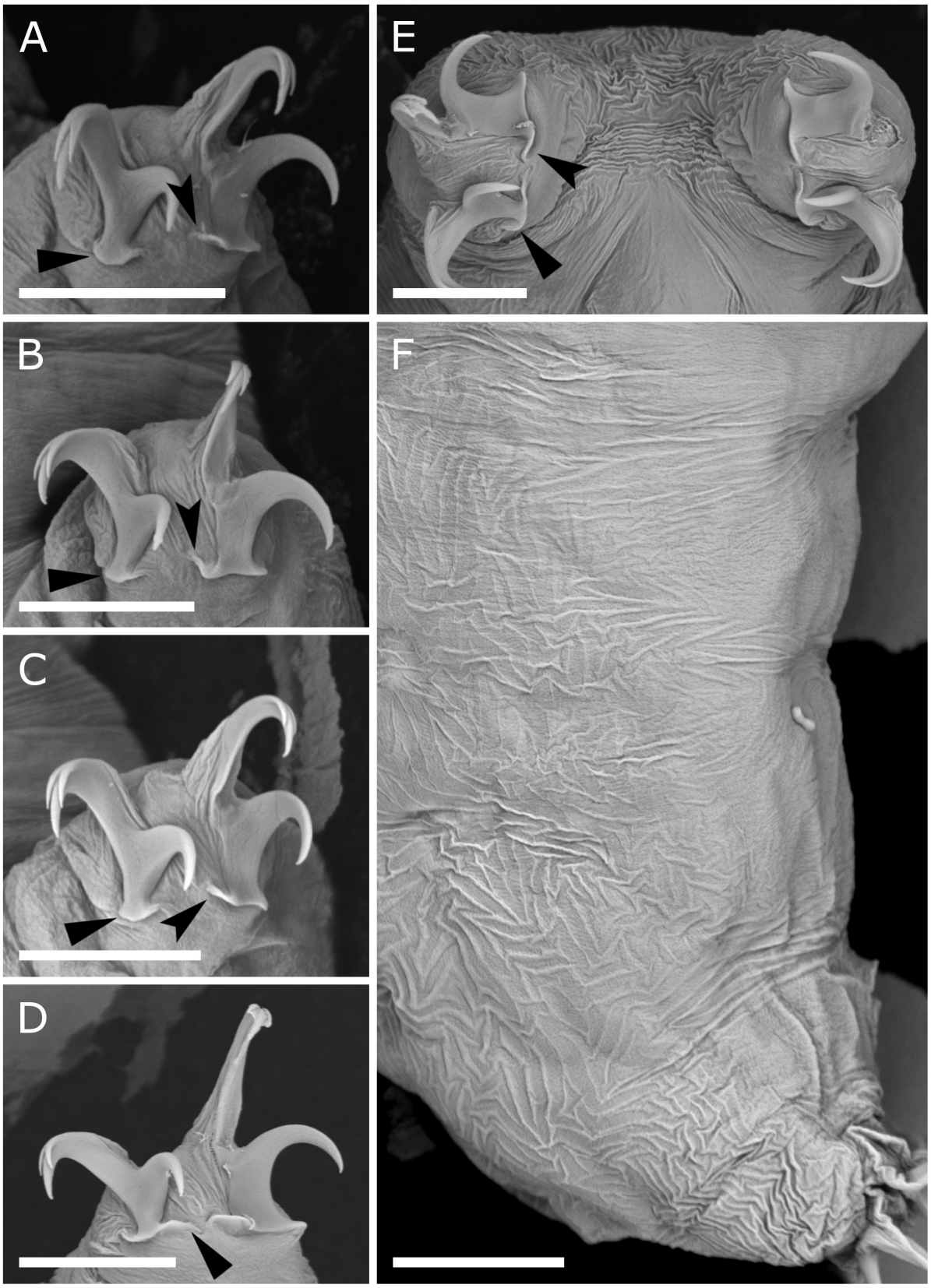

Fig. 11. *Fontourion secchii* (Bertolani & Rebecchi, 1996) from Italy, claws and body cuticle observed in SEM. (**A-D**) Claws I, II, III, and IV, respectively. (**E**) Hind legs with claws. (**F**) Cuticle in the caudo-lateral body region. Filled flat arrowheads indicate pseudolunulae, filled indented arrowheads indicate the cuticular thickening at the base of the external/posterior claw. Scale bar: 10 µm.

Eggs: The species lay roundish, smooth eggs, deposited in exuviae; however, they have not been found in our samples.

DNA sequences

We obtained sequences for all four of the above-mentioned molecular markers of the newly found population. Two individuals were sequenced for all four markers while third individual was sequence only for COI. DNA sequences are as follow: PX698780 and PX698779 (18S rRNA), PX698812 and PX698811 (28S rRNA), PX698829 and PX698828 (ITS-2), PX701220, PX701221 and PX701222 (COI).

Remarks

This species was found in three of the 35 samples analysed in this study (BOG.06.4, BOG.13.3, BOG.21.3; Supplementary Materials SM.05). The COI sequences of this species obtained in this study constitute the first COI barcodes for the family Microhypsibiidae (Surmacz *et al.*, 2025c). Up to now, only some sequences of 18S rRNA and 28S rRNA were available for the genus *Microhypsibius* (Bertolani *et al.*, 2014; Tumanov and Tsvetkova, 2023).

Discussion

Faunistic results

Our taxonomic inventory targeted tardigrades inhabiting poor fens, with some sites transitioning toward intermediate fen–bog complexes. The fauna recovered was strongly associated with aquatic or water-saturated habitats, which is consistent with the moisture-rich microhabitats we targeted during sampling. Most of the taxa identified in this study are considered hydrophilous in the literature. By combining detailed morphological analyses with DNA barcoding, we confirmed the presence of at least 30 species-level taxa. As noted in the Introduction, tardigrades in peat bogs and fens have been only sporadically studied, with the notable exception of recent work by Finnish researchers who examined tardigrade ecology using boreal peatlands as a study system (Mäenpää *et al.*, 2023, 2024, 2025). In their study, the authors reported 18 tardigrade genera occurring in boggy habitats (the same number of genera detected in our material) and 13 of these genera overlap with those recorded in our survey (Mäenpää *et al.*,

Tab. 6. Measurements (in µm) of selected morphological structures of individuals of *Microhypsibius minimus* Kristensen, 1982 from Italy mounted in Hoyer's medium.

Character	n	Range		Mean		SD	
		µm	*pt*	µm	*pt*	µm	*pt*
Body length	9	93–134	*618–842*	119	*753*	14	*82*
Buccal tube length	10	14.8–16.5	–	15.7	–	0.6	–
Stylet support insertion point	10	9.6–10.9	*63.7–68.4*	10.4	*66.1*	0.4	*1.8*
Buccal tube external width	10	1.2–1.7	*8.1–10.9*	1.5	*9.4*	0.1	*0.8*
Buccal tube internal width	9	0.7–0.9	*4.5–5.4*	0.8	*4.9*	0.1	*0.4*
Placoid lengths							
Macroplacoid 1	10	1.5–1.9	*9.7–12.3*	1.7	*11.1*	0.1	*0.9*
Macroplacoid 2	10	1.4–1.8	*9.1–11.6*	1.7	*10.5*	0.1	*0.8*
Macroplacoid 3	10	1.7–2.3	*11.3–14.1*	2.0	*12.7*	0.2	*0.7*
Septulum	10	0.6–1.1	*4.3–6.8*	0.9	*5.5*	0.1	*0.8*
Macroplacoid row	10	5.0–6.8	*33.5–42.5*	6.1	*38.8*	0.5	*2.3*
Placoid row	9	6.7–8.7	*44.7–54.0*	7.8	*49.5*	0.6	*2.6*
Claw I heights							
External primary branch	9	3.0–3.6	*19.4–22.5*	3.4	*21.4*	0.2	*1.0*
External secondary branch	5	2.1–2.6	*13.4–16.9*	2.4	*15.2*	0.2	*1.3*
Internal primary branch	8	2.6–3.5	*17.3–21.7*	3.1	*19.8*	0.3	*1.5*
Internal secondary branch	3	1.8–2.2	*11.4–13.4*	2.0	*12.1*	0.2	*1.1*
Claw II heights							
External primary branch	10	3.2–3.8	*20.7–24.0*	3.5	*22.1*	0.2	*1.2*
External secondary branch	10	2.1–2.8	*13.3–17.5*	2.5	*16.0*	0.2	*1.2*
Internal primary branch	7	3.0–3.4	*19.3–21.3*	3.2	*20.2*	0.1	*0.9*
Internal secondary branch	5	1.8–2.2	*11.6–14.4*	2.0	*12.7*	0.1	*1.0*
Claw III heights							
External primary branch	8	3.2–3.7	*20.5–23.1*	3.4	*21.8*	0.2	*0.9*
External secondary branch	9	2.4–3.0	*15.1–18.3*	2.6	*16.6*	0.2	*1.0*
Internal primary branch	7	3.1–3.4	*19.4–20.6*	3.2	*19.9*	0.1	*0.4*
Internal secondary branch	4	1.9–2.3	*12.5–13.8*	2.1	*13.2*	0.2	*0.5*
Claw IV heights							
Anterior primary branch	7	3.4–4.0	*22.6–25.4*	3.7	*24.0*	0.2	*1.1*
Anterior secondary branch	5	2.0–2.6	*13.7–16.4*	2.4	*15.3*	0.2	*1.1*
Posterior primary branch	7	3.7–4.5	*22.9–27.7*	4.0	*25.6*	0.3	*2.0*
Posterior secondary branch	6	3.0–3.5	*18.5–21.5*	3.2	*20.1*	0.2	*1.1*

n, number of specimens/structures measured; Range, refers to the smallest and the largest structure among all measured specimens; SD, standard deviation.

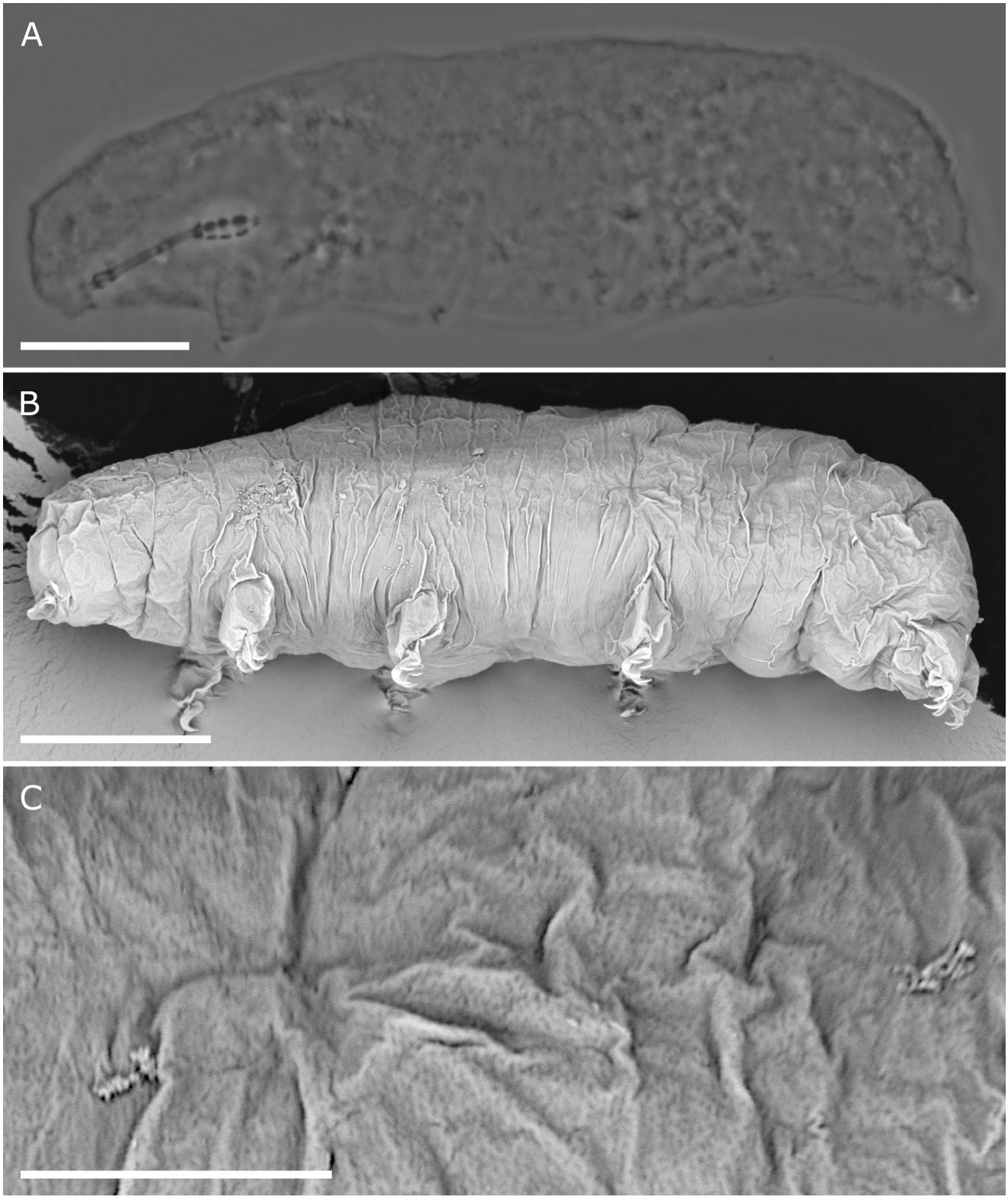

Fig. 12. *Microhypsibius minimus* Kristensen, 1982 from Switzerland, habitus and body cuticle observed in LM and SEM. (**A,B**) Habitus under PCM and SEM, respectively. (**C**) Dorso-caudal cuticle exhibiting minute ornamentation composed of small depressions forming a reticulate pattern. Scale bars: A,B) 20 µm; C) 5 µm.

2025). The most striking difference between the Finnish studies and our own lies in sampling strategy. Our work focused primarily on well-hydrated mosses, especially *Sphagnum*, whereas the Finnish studies sampled a broader diversity of bryophytes across landscape-level gradients of moisture retention. Consequently, it is not surprising that genera present in Finland but absent from our survey (*Mesocrista* Pilato, 1987, *Milnesium* Doyère, 1840, *Minibiotus* R.O. Schuster, 1980, *Platicrista* Pilato, 1987, *Ramazzottius* Binda & Pilato, 1986) are not typically regarded as freshwater or strongly hydrophilous taxa (Ramazzotti and Maucci, 1983; Dastych, 1988; Surmacz *et al.*, 2025b). Conversely, several genera recovered only in Italy (*Dianea* Gąsiorek, Stec, Morek & Michalczyk, 2019, *Arctodiphascon* Tumanov & Tsvetkova, 2023, *Microhypsibius*, *Fontourion*, *Cucumibius* Tumanov, Shunatova & Fedyuk, 2025, *Borealibius* Pilato, Guidetti, Rebecchi, Lisi, Hansen & Bertolani, 2006) are well known for their association with aquatic or rather moist microhabitats (Ramazzotti and Maucci, 1983; Dastych, 1988; Pilato *et al.*, 2006; Tumanov, 2025; Tumanov *et al.*, 2025).

Aside from the species that received detailed taxonomic and/or phylogenetic treatment (see above), several other taxa recovered in our survey also merit comment. One notable example is the discovery of *Cucumibius annulatus* (Murray, 1905), previously classified within *Grevenius* Gąsiorek, Stec, Morek & Michalczyk, 2019. Our specimens matched perfectly with published COI sequences of this species (Tumanov *et al.*, 2025). In their revision, (Tumanov *et al.*, 2025) examined *Grevenius annulatus* (Murray, 1905) from Lake Figurnoje (Russia) and transferred it to a newly erected genus *Cucumibius*, treating *Grevenius annulatus minor* (Ramazzotti, 1945) as its synonym. The latter taxon was originally described from the Bognanco valley (Ramazzotti, 1945), which is exactly one of our sampling areas. Given the large distance between the two populations (RU-IT; over 2000 km), and knowing that tardigrades show more localized distribution than previously thought (Morek *et al.*, 2021; Gąsiorek, 2024; Surmacz *et al.*, 2025a) one could suspect these populations could indeed represent different subspecies. However, our findings through DNA barcoding support the synonymy proposed by (Tumanov *et al.*, 2025) confirming a wide geographic range for this species which has been also found for several other tardigrades (e.g., Gąsiorek *et al.*, 2019; Kayastha *et al.*, 2023b, 2023a; Zawierucha *et al.*, 2023).

Another example of widely distributed species is *Borealibius zetlandicus*, which was also detected in our material, adding an

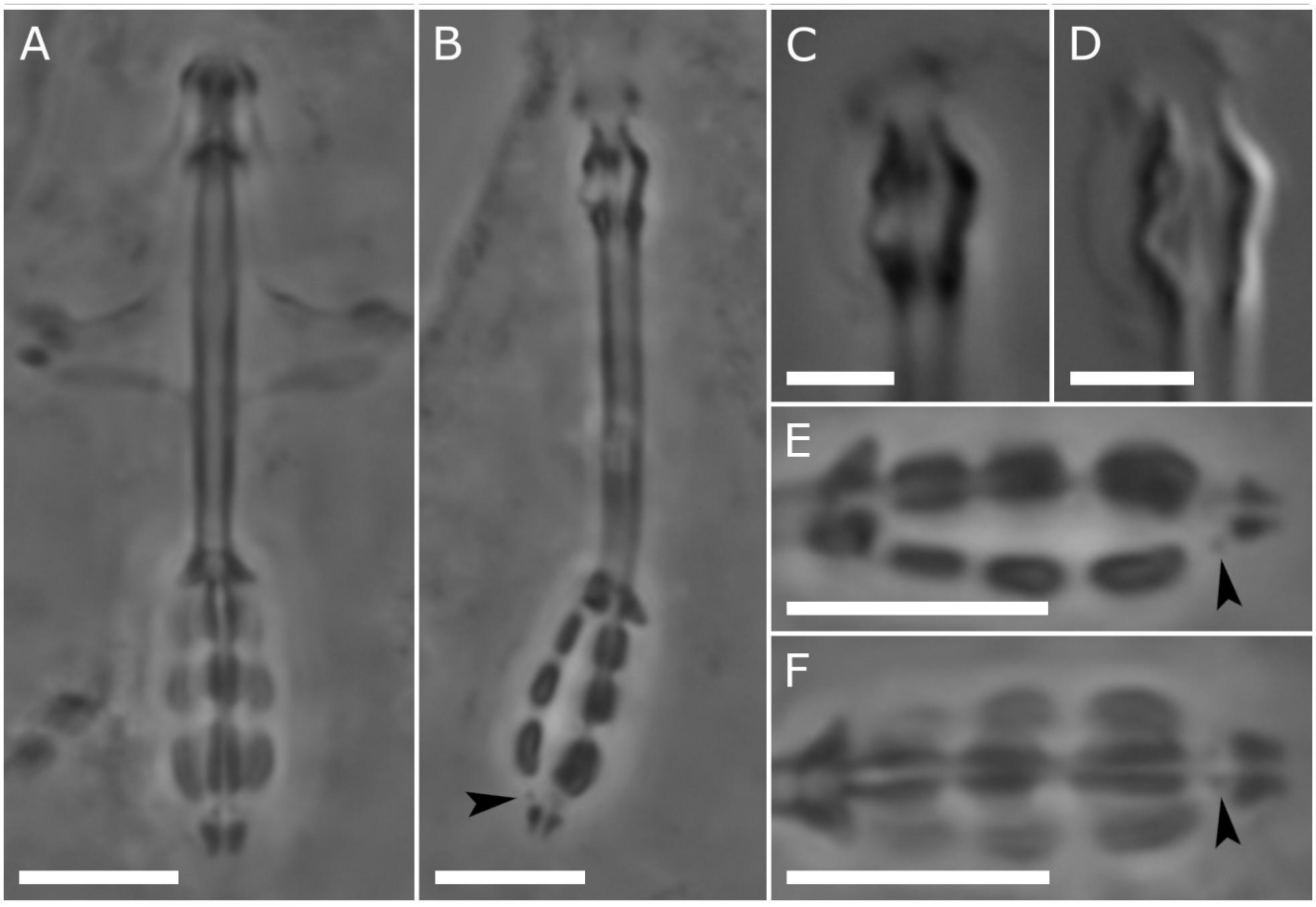

Fig. 13. *Microhypsibius minimus* Kristensen, 1982 from Switzerland, bucco-pharyngeal apparatus. (**A,B**) Entire bucco-pharyngeal apparatus, in ventral and lateral view, respectively (PCM). (**C,D**) AISM in lateral view, showing the ventral (left side) and dorsal (right side) crests (PCM and DIC, respectively). (**E,F**) Placoids in ventral and dorsal view, respectively (PCM). Filled indented arrowheads indicate faintly visible microplacoids. Scale bars: A,B,E,F) 5 µm; C,D) 2 µm.

important biogeographical element to the fauna of the sampled alpine fens. This species has a strikingly discontinuous distribution, occurring in polar, subpolar, and high-alpine environments above ~1,800 m asl (Pilato *et al.*, 2006) interpreted this pattern as characteristic of a boreo-alpine taxon and suggested that *Bor. zetlandicus* may represent a glacial relict in non-polar regions, persisting in cold, moisture-retaining microhabitats following post-glacial warming. Its presence in our alpine peatbog samples is therefore fully consistent with its known ecological preferences and supports the view that peatland microhabitats at high elevations can act as refugia for cold-adapted tardigrade lineages with boreo-alpine histories.

Arctodiphascon was detected in our study exclusively through DNA barcoding, as no specimens were available for detailed morphological examination. The COI sequence obtained matched the published sequence of *Arctodiphascon wuyingensis* (X.-L. Sun, J.-Y. Zhang, N. Wang, M. Zhao & Luo, 2020) from northern China with 96.8% similarity (GenBank Accession Number PP747645; Sun *et al.*, 2020). The geographic distance between our record and the type

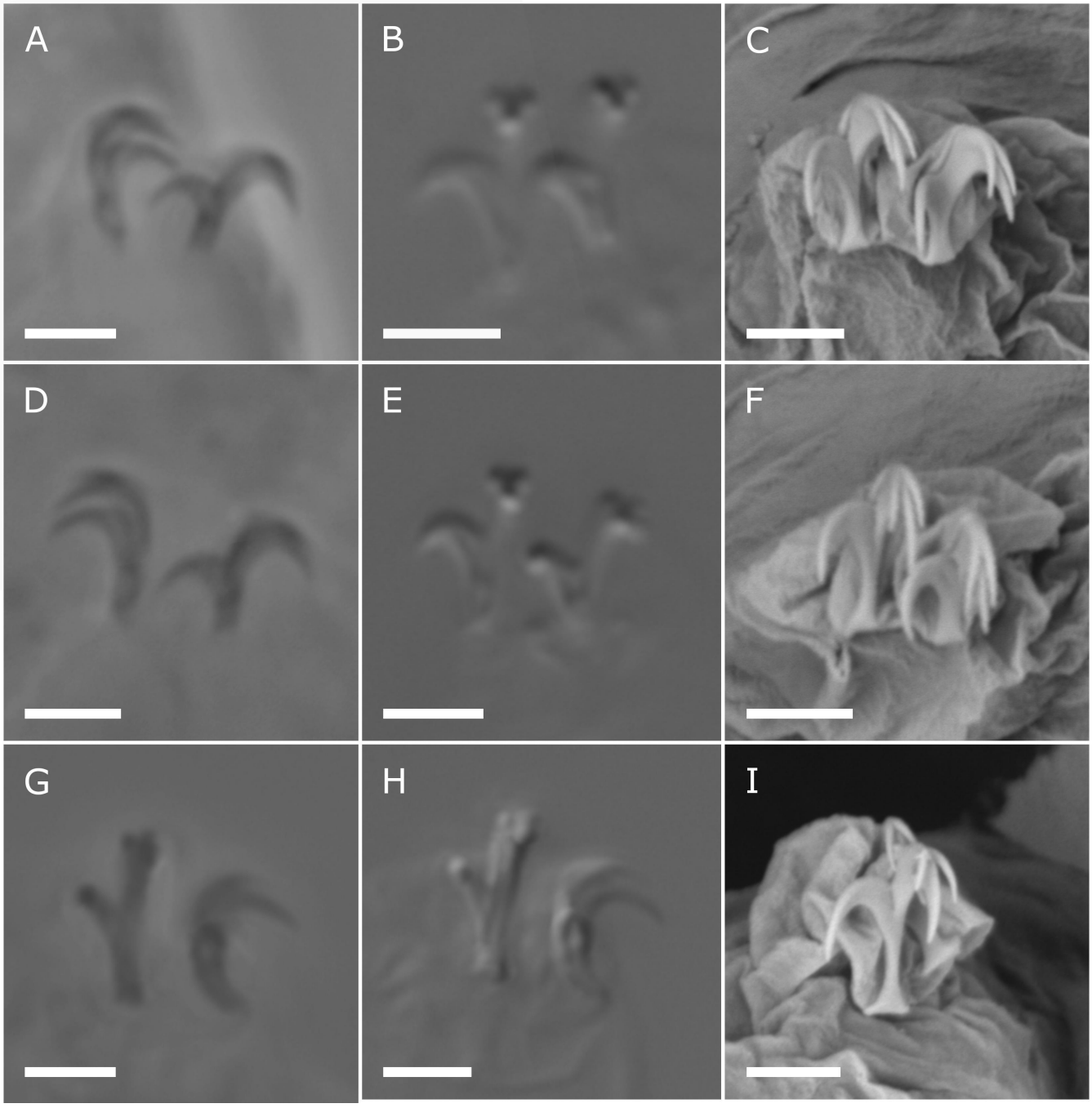

Fig. 14. *Microhypsibius minimus* Kristensen, 1982 from Switzerland, claws morphology. (**A-C**) Claws II under PCM, DIC and SEM, respectively. (**D-F**) Claws III under PCM, DIC and SEM, respectively. (**G-I**) Claws IV under PCM, DIC and SEM, respectively. Scale bars:2 µm.

locality is approximately 8,000 km. Although this level of similarity falls slightly below the commonly applied 97% threshold used in tardigrade DNA barcoding and metabarcoding (Cesari *et al.*, 2013; Surmacz *et al.*, 2025c), several studies have shown that intraspecific COI divergence in tardigrades can exceed 3% (Morek *et al.*, 2019; Stec *et al.*, 2022; Brandoli *et al.*, 2024). Given that our divergence value deviates only marginally from this conventional boundary, it is most plausible that the Italian and Chinese records represent the same species. Finally, our survey also recovered two examples of widely distributed taxa, *Macrobiotus hufelandi* and *Mac.* aff. *hufelandi*. These species are very common both in the study region (Surmacz *et al.*, 2025b) and globally (Surmacz *et al.*, 2025a). However, members of the genus *Macrobiotus* are not considered hydrophilous (Guidetti *et al.*, 2011); instead, they are typically associated with terrestrial mosses (Surmacz *et al.*, 2025b) and are well known for their strong cryptobiotic capabilities, particularly anhydrobiosis (Vecchi *et al.*, 2024; Stec *et al.*, 2025). Given their high abundance in surrounding terrestrial habitats and their preference for substrates drier than hydrophilous mosses such as *Sphagnum*, their presence in our fen samples is likely incidental.

Phylogenetic results and taxonomic treatments

The genus *Crenubiotus* currently comprises five described species, four of which are represented in our phylogeny (Fig. 1). The genus is relatively young, having been established only a few years ago (Lisi *et al.*, 2020) on the basis of distinctive morphological traits and subsequently confirmed through molecular evidence (Stec *et al.*, 2020c; Guidetti *et al.*, 2021). This history illustrates the power of integrative taxonomy and the value of redescribing older taxa (especially type species) in enabling the recognition of previously concealed diversity within morphologically similar lineages (Gąsiorek *et al.*, 2017; Kaczmarek *et al.*, 2018; Stec *et al.*, 2018, 2020b; Guidetti *et al.*, 2019; Grobys *et al.*, 2020; Stec, 2023). As noted in the Results, the published COI sequence attributed to the type species *Cre. crenulatus* is erroneous and likely derives from contamination. To date, the species described within *Crenubiotus* following the redescription of *Cre. crenulatus* have been morphologically well differentiated from one another, and extensive molecular species-delimitation analyses have not been essential for their diagnosis (Lisi *et al.*, 2020; Stec *et al.*, 2020c; Guidetti *et al.*, 2021; Vecchi *et al.*, 2022; Zhang *et al.*, 2024). However, our dataset already contains two genetically distinct but unidentified lineages within the genus, and the morphological differences among all *Crenubiotus* species described so far are relatively subtle. This suggests that more comprehensive species-delimitation work may become necessary as additional diversity within the genus is uncovered. Given that COI and ITS-2 remain the primary markers for species delimitation in tardigrade taxonomy, obtaining a reliable COI sequence from a new topotypic population of *Cre. crenulatus* would be particularly valuable for stabilising the taxonomy of the genus and for future integrative studies.

Our phylogenetic results for the family Murrayidae require broader comment, particularly regarding two issues. The first concerns the discrepancy between our findings and those of Camarda *et al.* (2025b) relating to the presence of two morphogroups within *Dactylobiotus*, differentiated by the presence or absence of dorsal papillae. In the phylogeny presented by Camarda *et al.* (2025b), these two morphogroups were recovered as distinct clades. In contrast, our results do not fully reflect this pattern: species lacking dorsal papillae (*Dac. octavi* and *Dac. ambiguus*) appear nested within the clade that Camarda *et al.* (2025b) considered to consist exclusively of species bearing dorsal papillae. However, this incongruence is most likely a phylogenetic artefact resulting from incomplete molecular representation. In our analyses, *Dac. octavi* and *Dac. ambiguus* are represented only by the highly conservative 18S rRNA marker. In contrast, Camarda *et al.* (2025b) excluded specimens for which only a single molecular marker was available, thereby basing their phylogeny on more informative multi-marker datasets. Given this limitation, caution is warranted when interpreting the position of *Dac. octavi* and *Dac. ambiguus* in our trees, and our results should not be taken as evidence contradicting the species circumscription of the *Dac. dispar* morphogroup proposed by Camarda *et al.* (2025b).

Guidetti *et al.* (2022) recently erected the genus *Paramurrayon* to accommodate a group of species within *Murrayon* that share the following diagnostic traits: three macroplacoids in the pharynx, pillar-like epicuticular structures visible under light microscopy, and eggs bearing chalice-shaped rod processes covered by a thin cuticular lamina ("blanket") connecting the distal ends of the rods to the egg surface. This taxonomic action preserved morphologically coherent and monophyletic genus-level groups and provided a more resolved classification than the alternative scenario of retaining all *Murrayon* taxa within a single, morphologically heterogeneous genus. However, *Murrayon hastatus* (Murray, 1907) has long represented an unresolved case. This species exhibits an unusual combination of characters: adult morphology consistent with *Murrayon* but egg morphology characteristic of *Paramurrayon*. As shown in our SEM images (Fig. 15), the eggs of *Mur. hastatus* differ strikingly from those of *Mur. pullari*, underscoring that the apparent similarity between *Murrayon*-like adults still conceals substantial morphological divergence. Guidetti *et al.* (2022) therefore placed it tentatively within *Murrayon*. More recently, Tumanov (2025) also documented the egg morphology of *Mur. hastatus* using SEM and suggested that more than one species may be present within the *Mur. hastatus* lineage. Until now, however, no molecular data were available for this taxon, preventing any test of its phylogenetic position relative to *Murrayon* and *Paramurrayon*. Our study provides the first molecular evidence addressing this problem. The results clearly show that *Murrayon*, as currently circumscribed, is polyphyletic: the taxa belonging to the *Mur. hastatus* lineage form a well-supported clade that is sister to *Paramurrayon*, rather than to other *Murrayon* species. This outcome implies two possible taxonomic solutions: (1) broadening the diagnosis of *Paramurrayon* to include *Mur. hastatus*, or (2) establishing a new genus for the *Mur. hastatus* lineage. At present, however, we refrain from proposing any formal changes. As noted earlier, linking adult and egg morphologies with confidence was not possible in our material due to the intermixing of lineages within samples, and the new morphological data provided by Tumanov (2025) are based solely on eggs. Until fully matched adult–egg associations and more complete morphological datasets become available, any taxonomic action would be premature. We therefore recommend caution and emphasize the need for integrative morphological and molecular data before the systematic position of *Mur. hastatus* is revised.

The genus *Fontourion* was recently established by Gąsiorek *et al.* (2024) to accommodate taxa previously placed in *Pilatobius* that possess a smooth cuticle. Its type species, *Fon. recamieri*, had been redescribed a few years earlier Gąsiorek *et al.* (2017). In that work, the authors were unable to identify any reliable morphological or morphometric characters separating *Fon. recamieri* from *Fon. secchii*, and consequently treated the latter as *species*

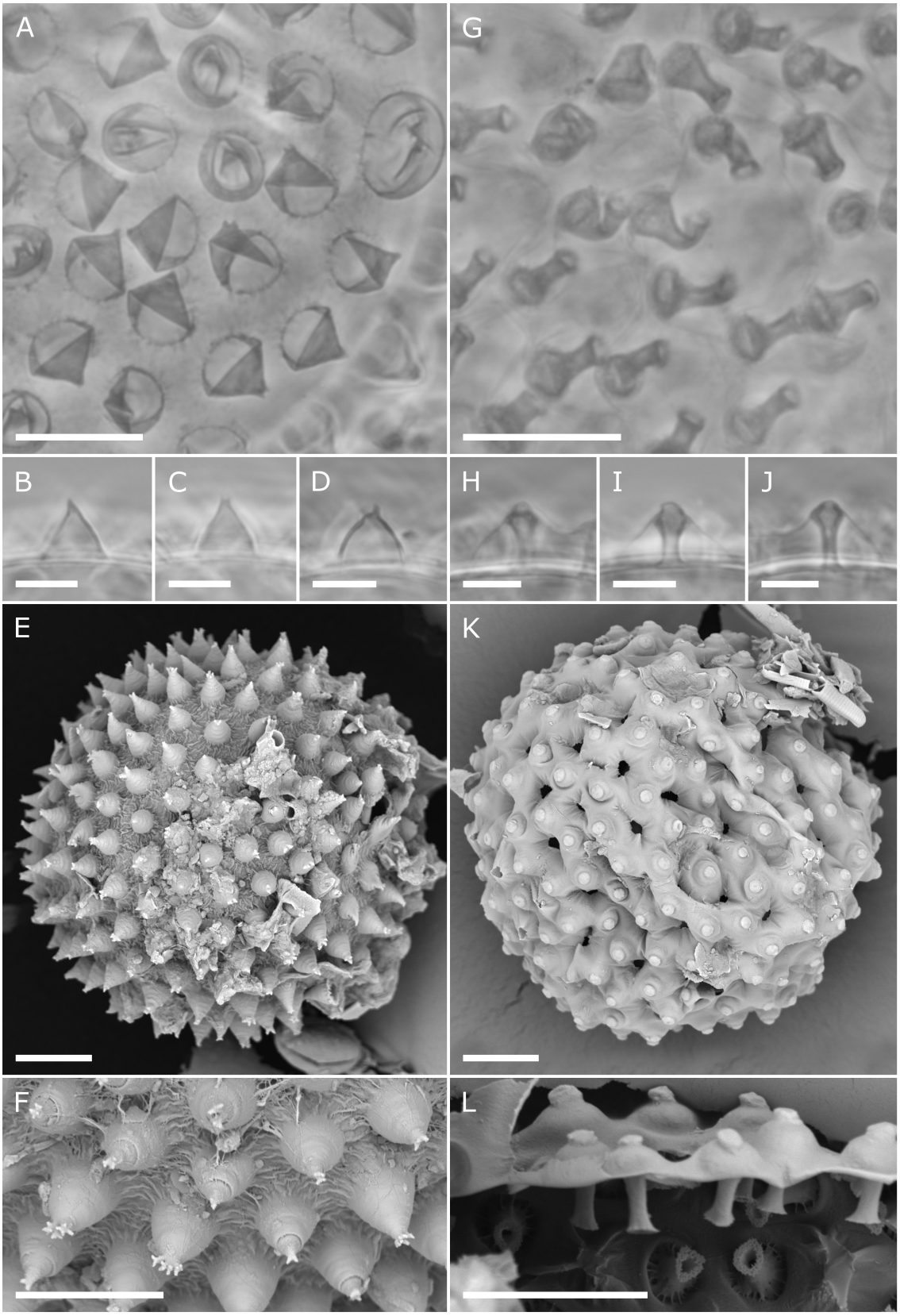

Fig. 15. *Murrayon* cf. *pullari* (**A-F**) and *Murrayon* cf. *hastatus* (**G-N**) from Italy, egg morphology. (**A,G**) Details of the egg shell and egg process surface observed in PCM. (**B-D, H-L**) Midsections of egg processes in PCM. (**E,M**) Entire egg observed in SEM. (**F, N**) Details of egg processes and egg shell surface observed in SEM. Scale bars: A,E,F,G,M,N) 10 µm; B-D, H-L) 5 µm.

inquirenda (Gąsiorek *et al.*, 2017). Subsequently, two additional *Fontourion* species were described, namely: *Fon. glaciale* (Zawierucha *et al.*, 2020) and *Fon. islandicum* (Buda *et al.*, 2018). Although these taxa are genetically well differentiated from *Fon. recamieri*, the morphological and morphometric distinctions among them remain extremely subtle (Gąsiorek *et al.*, 2017, 2024; Buda *et al.*, 2018; Zawierucha *et al.*, 2020; Janko *et al.*, 2024), effectively forming a cryptic species complex. The *Fontourion* population found in our study is clearly genetically distinct from all currently recognized congeners. We were unable to identify any consistent morphological differences not only between our material and the described species, but also between our specimens and the type material of *Fon. secchii*. Given that *Fon. secchii* was originally described from Monte Rondinaio in the Tusco-Emilian Apennines, approximately 290 km from our sampling site, we consider our population assignable to *Fon. secchii*. Based on the clear genetic separation from other sequenced *Fontourion* species, we further propose that *Fon. secchii* should be regarded as a valid species. However, because no molecular data are currently available from the type locality of *Fon. secchii*, the assignment of our population to this species should be regarded as provisional and hypothesis-driven. All currently recognized *Fontourion* taxa are known from cold northern or alpine regions, and the genus appears to consist of cold-adapted, largely boreo-alpine lineages. The occurrence of *Fontourion* in our high-elevation peatbog samples is therefore fully congruent with its known ecological affinities and biogeographic history.

The genus *Microhypsibius* has been reported only rarely, and available records suggest a disjunct boreo–alpine distribution. Confirmed occurrences include type localities of three species in northern regions (northern Scotland and Greenland; Thulin, 1928; Kristensen, 1982) and three records from alpine environments in Japan, Italy and Switzerland (Ito, 1995; Bertolani *et al.*, 2014; present study). Both morphological and molecular knowledge of the genus remains fragmentary, and all currently recognised species require integrative, modern redescriptions. At present, *Microhypsibius* comprises four species distinguished primarily by placoid configuration: species with three macroplacoids (*Mic. truncatus* Thulin, 1928); species with three macroplacoids and a microplacoid (*Mic. japonicus* Ito, 1991; *Mic. bertolanii* Kristensen, 1982); and a species with three macroplacoids, a microplacoid, and a septulum (*Mic. minimus* Kristensen, 1982). In this study, an Italian population of *Mic. minimus* was examined in detail, providing new morphological information and the first complete set of molecular markers for the genus. Morphological novelties concern the apophyses for the insertion of the stylet muscles (AISM), claw structure, and cuticular ultrastructure. Notably, the dorsal AISM was observed as an undivided crest, contrasting with the semilunar-hook configuration reported by Pilato and Binda (2010), while the ventral AISM appeared as an undulating crest with a more refractive medial portion rather than a ridge bearing a blunt hook. Additionally, the configuration of claw septa varied with viewing angle, appearing either as the primary branch inserted on the secondary branch or vice versa, differing from previous interpretations (Pilato, 1998; Pilato and Binda, 2010). Until now, molecular data for *Microhypsibius* were limited to a few specimens identified as *Mic. bertolanii* or *Mic.* cf. *bertolanii*, represented only by 18S and 28S rRNA sequences. This scarcity has prevented meaningful phylogenetic assessment of the genus and its monophyly. By providing the first complete molecular dataset for *Microhypsibius*, the present study establishes a foundation for future comparative analyses. Sequencing additional species representing different placoid configurations, combined with expanded morphological reassessment, will be essential to rigorously evaluate interspecific relationships and test the monophyly of the genus.

Conclusions

Our study combined morphological and molecular approaches to produce a comprehensive taxonomic survey of tardigrades inhabiting alpine fens in northern Italy. We documented a total of 30 species-level taxa and generated DNA barcodes for most of them. Because many of these taxa had not been sequenced previously, the newly generated barcodes substantially contribute to filling gaps in tardigrade reference databases, which are critical for reliable high-throughput biodiversity assessments such as DNA metabarcoding. This is particularly important in groups characterized by extensive cryptic diversity, a pattern also evident in our material, where several taxa could be distinguished only through genetic data. In addition, integrative taxonomic and phylogenetic analyses allowed us to i) describe a new species of *Crenubiotus*; ii) confirm the species validity of *Fon. secchii*; iii) provide new morphological and genetic data for the poorly known genus *Microhypsibius*; and iv) clarify the phylogenetic position of *Mur. hastatus* lineages, which had previously been only tentatively assigned to *Murrayon*. Together, these results underscore the value of integrating molecular evidence with classical taxonomy to resolve species boundaries and improve our understanding of tardigrade diversity in alpine ecosystems. Finally, our findings support the emerging view that alpine peatlands can act as microclimatic refugia for specialized and cold-adapted biota. Recent work has highlighted the role of peatlands as "open" and "wet–cool" islands within otherwise forested and warming landscapes, enabling the persistence of relict species far outside their continuous distributions (Słowińska *et al.*, 2026). The predominance of hydrophilous, boreo-alpine, and peatland-associated tardigrade taxa in our samples suggests that similar refugial mechanisms may also operate for microscopic metazoans. In this context, alpine peatlands may represent important reservoirs of hidden invertebrate diversity whose ecological and conservation significance has so far been largely overlooked.

References

Altschul SF, Gish W, Miller W, Myers EW, Lipman DJ, 1990. Basic local alignment search tool. J. Mol. Biol. 215:403–410.

Antala M, Juszczak R, Tol C van der, Rastogi A, 2022. Impact of climate change-induced alterations in peatland vegetation phenology and composition on carbon balance. Sci. Total Environ. 827:154294.

Beasley CW, Kaczmarek Ł, Michalczyk Ł, 2008. *Doryphoribius mexicanus*, a new species of Tardigrada (Eutardigrada: Hypsibiidae) from Mexico (North America). Proc. Biol. Soc. Wash. 121:34–40.

Bertolani R, Guidetti R, Marchioro T, Altiero T, Rebecchi L, Cesari M, 2014. Phylogeny of Eutardigrada: New molecular data and their morphological support lead to the identification of new evolutionary lineages. Mol. Phylogenet. Evol. 76:110–126.

Bertolani R, Rebecchi L, Giovannini I, Cesari M, 2011. DNA barcoding and integrative taxonomy of *Macrobiotus hufelandi*

C.A.S. Schultze 1834, the first tardigrade species to be described, and some related species. Zootaxa 2997:19–36.

Bielańska-Grajner I, Cudak A, Mieczan T, 2011. Epiphytic Rotifer Abundance and Diversity in Moss Patches in Bogs and Fens in the Polesie National Park (Eastern Poland). Int. Rev. Hydrobiol. 96:29–38.

Brandoli S, Cesari M, Massa E, Vecchi M, Rebecchi L, Guidetti R, 2024. Diverse eggs, diverse species? Production of two egg morphotypes in *Paramacrobiotus bifrons*, a new eutardigrade species within the areolatus group. Eur. Zool. J. 91:274–297.

Buda J, Olszanowski Z, Wierzgoń M, Zawierucha K, 2018. Tardigrades and oribatid mites in bryophytes from geothermally active lava fields (Krafla, Iceland) and the description of *Pilatobius islandicus* sp. nov. (Eutardigrada). Pol. Polar Res. 39:425–453.

Camacho C, Coulouris G, Avagyan V, Ma N, Papadopoulos J, Bealer K, Madden TL, 2009. BLAST+: architecture and applications. BMC Bioinformatics 10:421.

Camarda D, Lisi O, Stec D, Vecchi M, 2025a. Description of a new genus and species of Isohypsibioidea (Tardigrada), together with its mitochondrial genome sequence. Arthropod Syst. Phylogeny 83:427–445.

Camarda D, Massa E, Guidetti R, Lisi O, 2024. A new, simplified, drying protocol to prepare tardigrades for scanning electron microscopy. Microsc. Res. Tech. 87:716–726.

Camarda D, Pai C-Y, Kristensen RM, Stec D, 2025b. Integrative description of a new freshwater tardigrade species, *Dactylobiotus taiwanensis* (Tardigrada: Eutardigrada: Murrayidae), discovered through social media. Zool. Stud. 64:e14.

Casquet J, Thebaud C, Gillespie RG, 2012. Chelex without boiling, a rapid and easy technique to obtain stable amplifiable DNA from small amounts of ethanol-stored spiders. Mol. Ecol. Resour. 12:136–141.

Castresana J, 2000. Selection of conserved blocks from multiple alignments for their use in phylogenetic analysis. Mol. Biol. Evol. 17:540–552.

Cesari M, Giovannini I, Bertolani R, Rebecchi L, 2011. An example of problems associated with DNA barcoding in tardigrades: a novel method for obtaining voucher specimens. Zootaxa 3104:42–51.

Cesari M, Guidetti R, Rebecchi L, Giovannini I, Bertolani R, 2013. A DNA barcoding approach in the study of tardigrades. J. Limnol. 72:e23–e23.

Cowie RH, Bouchet P, Fontaine B, 2022. The Sixth Mass Extinction: fact, fiction or speculation? Biol. Rev. 97:640–663.

Dastych H, 1988. The Tardigrada of Poland. Monografie fauny Polski, Państwowe Wydawnictwo Naukowe, 255 pp.

Degma P, Guidetti R, 2025. Actual checklist of Tardigrada species. https://doi.org/10.25431/11380_1178608:

Flores-Romero RA, López-Sandoval D, Vincenzi J, Cesari M, Guidetti R, Dueñas-Cedillo A, Ruiz EA, Armendariz-Toledano F, 2025. A new *Diaforobiotus* species (Tardigrada: Eutardigrada: Richtersiusidae) from the Mexican transition zone, described based on multiple lines of evidence. Eur. Zool. J. 92:1171–1196.

Fontaneto D, Eckert EM, Anicic N, Lara E, Mitchell EAD, 2019. We are ready for faunistic surveys of bdelloid rotifers through DNA barcoding: the example of *Sphagnum* bogs of the Swiss Jura Mountains. Limnetica 38:213–225.

Garey JR, McInnes SJ, Nichols PB, 2008. Global diversity of tardigrades (Tardigrada) in freshwater. Hydrobiologia 595:101–106.

Gąsiorek P, 2024. Catch me if you can, or how paradigms of tardigrade biogeography evolved from cosmopolitism to 'localism.' Zool. J. Linn. Soc. 202:zlad191.

Gąsiorek P, Blagden B, Morek W, Michalczyk Ł, 2024. What is a 'strong' synapomorphy? Redescriptions of Murray's type species and descriptions of new taxa challenge the systematics of Hypsibiidae (Eutardigrada: Parachela). Zool. J. Linn. Soc. 202:zlad151.

Gąsiorek P, Michalczyk Ł, 2020. Phylogeny of Itaquasconinae in the light of the evolution of the flexible pharyngeal tube in Tardigrada. Zool. Scr. 49:499–515.

Gąsiorek P, Vončina K, Michalczyk Ł, 2019. Echiniscus testudo (Doyère, 1840) in New Zealand: anthropogenic dispersal or evidence for the 'Everything is Everywhere' hypothesis? N. Z. J. Zool. 46:174–181.

Gąsiorek P, Zawierucha K, Stec D, Michalczyk Ł, 2017. Integrative redescription of a common Arctic water bear *Pilatobius recamieri* (Richters, 1911). Polar Biol. 40:2239–2252.

Grobys D, Roszkowska M, Gawlak M, Kmita H, Kepel A, Kepel M, Parnikoza I, Bartylak T, Kaczmarek Ł, 2020. High diversity in the *Pseudechiniscus suillus–facettalis* complex (Heterotardigrada: Echiniscidae) with remarks on the morphology of the genus *Pseudechiniscus*. Zool. J. Linn. Soc. 188:733–752.

Guidetti R, Altiero T, Bertolani R, Grazioso P, Rebecchi L, 2011. Survival of freezing by hydrated tardigrades inhabiting terrestrial and freshwater habitats. Zoology 114:123–128.

Guidetti R, Cesari M, Bertolani R, Altiero T, Rebecchi L, 2019. High diversity in species, reproductive modes and distribution within the *Paramacrobiotus richtersi* complex (Eutardigrada, Macrobiotidae). Zool. Lett. 5:1.

Guidetti R, Giovannini I, Del Papa V, Ekrem T, Nelson DR, Rebecchi L, Cesari M, 2022. Phylogeny of the asexual lineage Murrayidae (Macrobiotoidea, Eutardigrada) with the description of *Paramurrayon* gen. nov. and *Paramurrayon meieri* sp. nov. Invertebr. Syst. 36:1099–1117.

Guidetti R, Rebecchi L, Bertolani R, Jönsson KI, Møbjerg Kristensen R, Cesari M, 2016. Morphological and molecular analyses on *Richtersius* (Eutardigrada) diversity reveal its new systematic position and lead to the establishment of a new genus and a new family within Macrobiotoidea. Zool. J. Linn. Soc. 178:834–845.

Guidetti R, Rizzo AM, Altiero T, Rebecchi L, 2012. What can we learn from the toughest animals of the Earth? Water bears (tardigrades) as multicellular model organisms in order to perform scientific preparations for lunar exploration. Planet. Space Sci. 74:97–102.

Guidetti R, Schill RO, Giovannini I, Massa E, Goldoni SE, Ebel C, Förschler MI, Rebecchi L, Cesari M, 2021. When DNA sequence data and morphological results fit together: Phylogenetic position of *Crenubiotus* within Macrobiotoidea (Eutardigrada) with description of *Crenubiotus ruhesteini* sp. nov. J. Zool. Syst. Evol. Res. 59:576–587.

Hoang DT, Chernomor O, Haeseler A von, Minh BQ, Vinh LS, 2018. UFBoot2: improving the ultrafast bootstrap approximation. Mol. Biol. Evol. 35:518–522.

Ito M, 1995. Taxonomic Study on the Eutardigrada from the Northern Slope of Mt. Fuji, Central Japan, II. Family Hypsibiidae. Proc. Jpn. Soc. Syst. Zool. 53:18–39.

Janko K, Shain DH, Fontaneto D, Kaštánková Doležálková M, Buda J, Štefková Kašparová E, Šabacká M, Rosvold J, Stefaniak J,

Hessen DO, Devetter M, Jimenez/Santos MA, et al., 2024. Islands of ice: Glacier-dwelling metazoans form regionally distinct populations despite extensive periods of deglaciation. Divers. Distrib. 30:e13859.

Kaczmarek Ł, Cytan J, Zawierucha K, Diduszko D, Michalczyk Ł, 2014. Tardigrades from Peru (South America), with descriptions of three new species of Parachela. Zootaxa 3790:357–379.

Kaczmarek Ł, Michalczyk Ł, 2017. The *Macrobiotus hufelandi* group (Tardigrada) revisited. Zootaxa 4363:101–123.

Kaczmarek Ł, Zawierucha K, Buda J, Stec D, Gawlak M, Michalczyk Ł, Roszkowska M, 2018. An integrative redescription of the nominal taxon for the *Mesobiotus harmsworthi* group (Tardigrada: Macrobiotidae) leads to descriptions of two new *Mesobiotus* species from Arctic. PLOS ONE 13: e0204756.

Katoh K, Misawa K, Kuma K, Miyata T, 2002. MAFFT: a novel method for rapid multiple sequence alignment based on fast Fourier transform. Nucleic Acids Res. 30:3059–3066.

Katoh K, Standley DM, 2013. MAFFT Multiple Sequence Alignment Software Version 7: Improvements in Performance and Usability. Mol. Biol. Evol. 30:772–780.

Kayastha P, Stec D, Sługocki Ł, Gawlak M, Mioduchowska M, Kaczmarek Ł, 2023a. Integrative taxonomy reveals new, widely distributed tardigrade species of the genus Paramacrobiotus (Eutardigrada: Macrobiotidae). Sci. Rep. 13:2196.

Kayastha P, Szydło W, Mioduchowska M, Kaczmarek Ł, 2023b. Morphological and genetic variability in cosmopolitan tardigrade species—Paramacrobiotus fairbanksi Schill, Förster, Dandekar & Wolf, 2010. Sci. Rep. 13:17672.

Kayastha P, Wiśniewska J, Kuzdrowska K, Kaczmarek Ł, Kayastha P, Wiśniewska J, Kuzdrowska K, Kaczmarek Ł, 2021. Aquatic Tardigrades in Poland—A review. Limnol. Rev. 21:147–154.

Kiosya Y, Pogwizd J, Matsko Y, Vecchi M, Stec D, 2021. Phylogenetic position of two *Macrobiotus* species with a revisional note on *Macrobiotus sottilei* Pilato, Kiosya, Lisi & Sabella, 2012 (Tardigrada: Eutardigrada: Macrobiotidae). Zootaxa 4933:113–135.

Kisielewska G, 1982. Gastrotricha of two complexes of peat hags near Siedlce. Fragm. Faun. 27:39–57.

Kisielewski J, 1981. Gastrotricha from Raised and Transitional Peat Bogs in Poland. Monografie fauny Polski, Polska Akademia Nauk, Kraków: 143 pp.

Kosztyła P, Stec D, Morek W, Gąsiorek P, Zawierucha K, Michno K, Ufir K, Małek D, Hlebowicz K, Laska A, Dudziak M, Frohme M, et al., 2016. Experimental taxonomy confirms the environmental stability of morphometric traits in a taxonomically challenging group of microinvertebrates. Zool. J. Linn. Soc. 178:765–775.

Kristensen RM, 1982. New aberrant eutardigrades from homothermic springs on Disko Island, West Greenland, p. 203–220 In: Proceedings of the Third International Symposium on Tardigrada, Tennessee 1980, Johnson City, Tennessee: East Tennessee State University Press.

Kumar S, Stecher G, Suleski M, Sanderford M, Sharma S, Tamura K, 2024. MEGA12: Molecular Evolutionary Genetic Analysis Version 12 for Adaptive and Green Computing. Mol. Biol. Evol. 41.

Lanfear R, Frandsen PB, Wright AM, Senfeld T, Calcott B, 2017. PartitionFinder 2: new methods for selecting partitioned models of evolution for molecular and morphological phylogenetic analyses. Mol. Biol. Evol. 34:772–773.

Lisi O, Londoño R, Quiroga S, 2020. Description of a new genus and species (Eutardigrada: Richtersiidae) from Colombia, with comments on the family Richtersiidae. Zootaxa 4822:531–550.

Mäenpää H, Elo M, Calhim S, 2024. A first look into moss living tardigrades in boreal peatlands. Ecol. Evol. 14:e70045.

Mäenpää H, Elo M, Kotiaho JS, Meriläinen E, Calhim S, 2025. Tardigrade communities in pristine, drained and restored pine mire forests. BMC Ecol. Evol. 25:126.

Mäenpää H, Elo M, Vuori T, Calhim S, 2023. The effects of sample storage duration on tardigrade density and community composition in moss samples. Pedobiologia 99–100:150895.

Martínez A, Bonaglia S, Di Domenico M, Fonseca G, Ingels J, Jörger KM, Laumer C, Leasi F, Zeppilli D, Baldrighi E, Bik H, Cepeda D, et al., 2025. Fundamental questions in meiofauna research highlight how small but ubiquitous animals can improve our understanding of Nature. Commun. Biol. 8:1–17.

Massa E, Vecchi M, Calhim S, Choong H, 2024. First records of limnoterrestrial tardigrades (Tardigrada) from Haida Gwaii, British Columbia, Canada. Eur. Zool. J. 91:1–20.

McFatter MM, Meyer HA, Hinton JG, 2007. Nearctic freshwater tardigrades: a review. J. Limnol. 66:84.

Michalczyk Ł, Kaczmarek Ł, 2013. The Tardigrada Register: a comprehensive online data repository for tardigrade taxonomy. J. Limnol. 72:e22–e22.

Moore PD, 2002. The future of cool temperate bogs. Environ. Conserv. 29:3–20.

Morek W, Stec D, Gąsiorek P, Surmacz B, Michalczyk Ł, 2019. *Milnesium tardigradum* Doyère, 1840: The first integrative study of interpopulation variability in a tardigrade species. J. Zool. Syst. Evol. Res. 57:1–23.

Morek W, Surmacz B, López-López A, Michalczyk Ł, 2021. "Everything is not everywhere": Time-calibrated phylogeography of the genus *Milnesium* (Tardigrada). Mol. Ecol. 30:3590–3609.

Nelson DR, Guidetti R, Rebecchi L, 2019. Chapter 15 - Phylum Tardigrada, p. 533–548 In: Rogers DC and JH Thorp (eds.), Thorp and Covich's Freshwater Invertebrates (Fourth Edition), Boston: Academic Press.

Nguyen L-T, Schmidt HA, Haeseler A von, Minh BQ, 2015. IQ-TREE: a fast and effective stochastic algorithm for estimating maximum-likelihood phylogenies. Mol. Biol. Evol. 32:268–274.

Nielsen C, 2011. PANARTHROPODA, p. 0 In: Nielsen C (ed.), Animal Evolution: Interrelationships of the Living Phyla, Oxford University Press.

Nordbeck R, Hogl K, 2023. National peatland strategies in Europe: current status, key themes, and challenges. Reg. Environ. Change 24:5.

Perry E, Miller WR, Kaczmarek Ł, 2019. Recommended abbreviations for the names of genera of the phylum Tardigrada. Zootaxa 4608:zootaxa.4608.1.8.

Pilato G, 1981. Analisi di nuovi caratteri nello studio degli Eutardigradi. Animalia 8:51–57.

Pilato G, 1998. Microhypsibiidae, new family of eutardigrades, and description of the new genus *Fractonotus*. Spixiana 21:129–134.

Pilato G, Binda MG, 2010. Definition of families, subfamilies, genera and subgenera of the Eutardigrada, and keys to their identification. Zootaxa 2404:1–54.

Pilato G, Guidetti R, Rebecchi L, Lisi O, Hansen JG, Bertolani R, 2006. Geonemy, ecology, reproductive biology and morphology of the tardigrade *Hypsibius zetlandicus* (Eutardigrada:

Hypsibiidae) with erection of *Borealibius* gen. n. Polar Biol. 29:595–603.
Puillandre N, Brouillet S, Achaz G, 2021. ASAP: assemble species by automatic partitioning. Mol. Ecol. Resour. 21:609–620.
Ramazzotti G, 1945. Nuovi Tardigradi della fauna italiana. Atti Della Soc. Ital. Sci. Nat. 84:98–104.
Ramazzotti G, Maucci M, 1983. Il Phylum Tardigrada. Memorie dell'Istituto Italiano di Idrobiologia, Verbania Pallanza: 1012 pp.
Rambaut A, Drummond AJ, Xie D, Baele G, Suchard MA, 2018. Posterior summarization in bayesian phylogenetics using Tracer 1.7. Syst. Biol. 67:901–904.
Renčo M, Janko K, Devetter M, 2025. Coupling between plants and nematode community in high arctic tundra soil. Polar Biol. 48:104.
Ronquist F, Huelsenbeck JP, 2003. MrBayes 3: Bayesian phylogenetic inference under mixed models. Bioinformatics 19:1572–1574.
Rowland JA, Bracey C, Moore JL, Cook CN, Bragge P, Walsh JC, 2021. Effectiveness of conservation interventions globally for degraded peatlands in cool-climate regions. Biol. Conserv. 263:109327.
Rydin H, Jeglum JK, 2006. Peatland habitats, p. 0 In: Rydin H and JK Jeglum (eds.), The Biology of Peatlands, Oxford University Press.
Sayers EW, Bolton EE, Fine AM, Kelly C, Kim S, Landrum M, Lathrop S, Malheiro A, Murphy TD, Phan L, Pujar S, Trawick BW, et al., 2026. Database resources of the National Center for Biotechnology Information in 2026. Nucleic Acids Res. 54:D20–D27.
Słowińska S, Ronikier M, Paul W, Kaszkiel A, Kowalczyk P, Słowiński M, 2026. The role of microclimate in supporting peatlands as climate-change refugia: A Central European perspective. Conserv. Sci. Pract. n/a:e70172.
Stec D, 2023. Integrative taxonomy helps to revise systematics and questions the purported cosmopolitan nature of the type species within the genus *Diaforobiotus* (Eutardigrada: Richtersiusidae). Org. Divers. Evol. 23:309–328.
Stec D, Kristensen RM, Michalczyk Ł, 2020a. An integrative description of *Minibiotus ioculator* sp. nov. from the Republic of South Africa with notes on *Minibiotus pentannulatus* Londoño et al., 2017 (Tardigrada: Macrobiotidae). Zool. Anz. 286:117–134.
Stec D, Krzywański Ł, Zawierucha K, Michalczyk Ł, 2020b. Untangling systematics of the *Paramacrobiotus areolatus* species complex by an integrative redescription of the nominal species for the group, with multilocus phylogeny and species delineation in the genus *Paramacrobiotus*. Zool. J. Linn. Soc. 188:694–716.
Stec D, Morek W, 2022. Reaching the Monophyly: Re-Evaluation of the Enigmatic species *Tenuibiotus hyperonyx* (Maucci, 1983) and the genus *Tenuibiotus* (Eutardigrada). Animals 12:404.
Stec D, Morek W, Gąsiorek P, Michalczyk Ł, 2018. Unmasking hidden species diversity within the *Ramazzottius oberhaeuseri* complex, with an integrative redescription of the nominal species for the family Ramazzottiidae (Tardigrada: Eutardigrada: Parachela). Syst. Biodivers. 16:357–376.
Stec D, Vecchi M, Budzik K, Matsko Y, Miler K, 2025. Distribution of tardigrade cryptobiotic abilities across a fine-scale habitat gradient. Org. Divers. Evol. 25:43–54.
Stec D, Vecchi M, Calhim S, Michalczyk Ł, 2021. New multilocus phylogeny reorganises the family Macrobiotidae (Eutardigrada) and unveils complex morphological evolution of the *Macrobiotus hufelandi* group. Mol. Phylogenet. Evol. 160: 106987.
Stec D, Vecchi M, Maciejowski W, Michalczyk Ł, 2020c. Resolving the systematics of Richtersiidae by multilocus phylogeny and an integrative redescription of the nominal species for the genus *Crenubiotus* (Tardigrada). Sci. Rep. 10:19418.
Stec D, Vončina K, Møbjerg Kristensen R, Michalczyk Ł, 2022. The *Macrobiotus ariekammensis* species complex provides evidence for parallel evolution of claw elongation in macrobiotid tardigrades. Zool. J. Linn. Soc. 195:1067–1099.
Sun X-L, Zhang J-Y, Wang N, Zhao M, Luo X-G, 2020. A new species of *Diphascon* (Tardigrada: Hypsibiidae) from Northern China supported by integrated taxonomy. Zootaxa 4722:185–194.
Surmacz B, Budzik K, Matsko Y, Stec D, 2025a. Human impact on microinvertebrate diversity and distributions: questioning the resilience of tardigrades. Glob. Ecol. Biogeogr. 34:e70167.
Surmacz B, Fontaneto D, Vončina G, Stec D, 2025b. Deciphering the patterns and drivers of tardigrade diversity along altitudinal gradients. Mol. Ecol. 34:e70196.
Surmacz B, Vecchi M, Fontaneto D, Budzik K, Godziek J, Matsko Y, Stec D, 2025c. COI metabarcoding with a curated reference database and optimized protocol provides a reliable species-level diversity assessment of tardigrades. Integr. Zool.
The GIMP Development Team, 2019.
Thulin G, 1928. Über die phylogenie und das system der tardigraden. Hereditas 11:207–266.
Trifinopoulos J, Nguyen L-T, von Haeseler A, Minh BQ, 2016. W-IQ-TREE: a fast online phylogenetic tool for maximum likelihood analysis. Nucleic Acids Res. 44:W232–W235.
Tumanov DV, 2025. Set to its place: first DNA data on freshwater tardigrades of Sakhalin (Far East Russia) shed light on the phylogenetic position of *Mixibius* (Eutardigrada: Hypsibioidea). 2025.11.28.691205.
Tumanov DV, Shunatova NN, Fedyuk KA, 2025. Integrative description of *Grevenius annulatus* (Eutardigrada, Isohypsibioidea) from North-West Russia with new data on the species cuticular structure leads to the institution of a new genus. Zool. Scr. 54:232–252.
Tumanov DV, Tsvetkova AYu, 2023. Some have drops and some do not, but can we rely on that? Re-investigation of *Diphascon tenue* (Tardigrada: Eutardigrada) with discussion of the phylogeny and taxonomy of the superfamily Hypsibioidea. Zoosystematica Ross. 32:50–74.
Vaidya G, Lohman DJ, Meier R, 2011. SequenceMatrix: concatenation software for the fast assembly of multi-gene datasets with character set and codon information. Cladistics 27:171–180.
Vecchi M, Choong H, Calhim S, 2022. A new species of the genus *Crenubiotus* (Tardigrada: Eutardigrada: Adorybiotidae) from Salt Spring Island, strait of Georgia, British Columbia (Canada). Folia Biol. (Praha) 70:93–105.
Vecchi M, Godziek J, Kristensen RM, Piemontese L, Calhim S, Stec D, 2025. Taxonomic reanalysis of the genus *Richtersius* (Tardigrada; Eutardigrada), with description of two new species from Italy and Sweden. Eur. J. Taxon. 981:155–188.
Vecchi M, Stec D, Rebecchi L, Michalczyk Ł, Calhim S, 2024. Ecology explains anhydrobiotic performance across tardigrades, but the shared evolutionary history matters more. J. Anim. Ecol. 93:307–318.

Wełnicz W, Grohme MA, Kaczmarek L, Schill RO, Frohme M, 2011. Anhydrobiosis in tardigrades—the last decade. J. Insect Physiol. 57:577–583.

Wu R, Pisani D, Donoghue PCJ, 2023. The unbearable uncertainty of panarthropod relationships. Biol. Lett. 19:20220497.

Zawierucha K, Buda J, Jaromerska TN, Janko K, Gąsiorek P, 2020. Integrative approach reveals new species of water bears (*Pilatobius*, *Grevenius*, and *Acutuncus*) from Arctic cryoconite holes, with the discovery of hidden lineages of *Hypsibius*. Zool. Anz. 289:141–165.

Zawierucha K, Kašparová EŠ, McInnes S, Buda J, Ambrosini R, Devetter M, Ficetola GF, Franzetti A, Takeuchi N, Horna P, Jaroměřská TN, Ono M, et al., 2023. Cryophilic Tardigrada have disjunct and bipolar distribution and establish long-term stable, low-density demes. Polar Biol. 46:1011–1027.

Zhang J-Y, Sun X-L, Wang N, Hao L, Ma C-X, Zhao N, Li H-P, Zhao M, Yang S-T, 2024. Tardigrades in the alpine region of Northeast China with an integrative description of *Crenubiotus liangshuiensis* sp. nov. Zootaxa 5492:96–108.

Online supplementary material:

SM.01. Raw morphometric data underling the description of Crenubiotus meg *sp. nov.*

SM.02. Raw morphometric data underling the description of Fontourion secchi *from Italy.*

SM.03. Raw morphometric data underling the description of Microhypsibius minimus *from Switzerland.*

SM.04. Supplementary information containing: (i) primers and PCR programs used in this study, (ii) GenBank Accession Numbers for DNA sequences obtained in this study, (iii) concatenation table containing GenBank Accession Numbers used in the phylogenetic analyses, (iv) raw phylogenetic trees in newick format.

SM.05. Supplementary information containing: (i) results of ASAP delimitation analysis, (ii) results of BLASTn searches (perfect matches), (iii) p-distances and NJ-tree of four Fontourion *taxa, (iv) table with faunistic information of morphologically identified specimens mounted in permanent slides, (v) table with presence / absence data of each species found in this study per analysed sample.*

SM.06. Supplementary figures S1-S3: (S1) map with five sampling areas, (S2) morphology of the rotifer egg, (S3) Fontourion secchi *– holotype.*

Received: 3 February 2026; Accepted: 9 March 2026.

Edited by: Michela Rogora, *CNR-IRSA Water Research Institute, Verbania-Pallanza, Italy.*

Citation: Camarda A, Fontaneto D, Bajorek D, Lisi O, Stec D. Taxonomic survey and DNA barcode library of tardigrades from alpine fens in northwestern Italy. *J Limnol 2026;85:2262.*

Acknowledgements: We would like to express our gratitude to Grzegorz Vončina for identifying mosses, to Matteo Vecchi for his help in initial phase of photo-vouchering part of the investigated specimens and to Roberto Guidetti for providing us with photographs of *Fontourion secchi* and to Lyudmila Kamburska for her help in uploading dataset to GBIF. We thank the protected area Aree Protette dell'Ossola that provided us with sampling permits, Permit n. 0001592/2023. Daniel Stec was supported by the Polish National Agency for Academic Exchange (Bekker scholarship, number BPN/BEK/2024/1/00101). This work and the new species name have been registered with ZooBank under urn:lsid:zoobank.org:pub:15E0EFCF-6201-4CF6-A2AC-2C821AE72E6F.

CRediT authorship contribution statement: Daniele Camarda, investigation, conceptualization, writing – review & editing; methodology, data curation; Diego Fontaneto, field work, resources, writing – review & editing; Daniel Bajorek, field work, investigation, writing – review & editing; Oscal Lisi, resources, investigation, writing – review & editing; Daniel Stec, investigation, conceptualization, writing – original draft, writing – review & editing, Formal analysis, visualization, supervision, resources, validation, project administration.

Conflict of interest: the authors declare that they have no known competing financial interests or personal relationships that could have appeared to influence the work reported in this paper.

Funding: the survey was supported by the National Biodiversity Future Centre (NBFC) funded by the Italian Ministry of University and Research, PNRR, Missione 4 Componente 2, "Dalla ricerca all'impresa", Investimento 1.4, Project CN00000033, CUP B83C22002930006.

Availability of data: the nucleotide sequence data reported are available in the GenBank under accession numbers PX701207-PX701251, PX698770-PX698801, PX698802-PX698820, PX698822-PX698837, All other data generated or analysed during this study are included in this published article and its supplementary information files. The datasets of moss and of tardigrade occurrences are available as GBIF datasets: https://doi.org/10.15468/x4wnb6 and https://doi.org/10.15468/fbkkvp.

Declaration of generative AI and AI-assisted technologies in the manuscript preparation process

During the preparation of this work, the authors used ChatGPT in order to improve the readability and language of the manuscript. After using this tool, the authors reviewed and edited the content as needed and took full responsibility for the content of the published article.